CHALMERS
UNIVERSITY OF TECHNOLOGY

DEM Modeling of Snow-Wall Adhesion

Development of a particle stick or bounce regime map for prediction of snow accumulation on cars

Master's thesis in the program Innovative and Sustainable Chemical Engineering

ANDERS LIND

Department of Chemistry and Chemical Engineering
CHALMERS UNIVERSITY OF TECHNOLOGY
Gothenburg, Sweden 2017

THESIS FOR THE DEGREE MASTER OF SCIENCE

DEM Modeling of Snow-Wall Adhesion

Development of a particle stick or bounce regime map for prediction of snow accumulation on cars

ANDERS LIND

Chemical Engineering
Department of Chemistry and Chemical Engineering
CHALMERS UNIVERSITY OF TECHNOLOGY
Gothenburg, Sweden 2017

DEM MODELING OF SNOW-WALL ADHESION

Development of a particle stick or bounce regime map for prediction of snow accumulation on cars

ANDERS LIND

Department of Chemistry and Chemical Engineering
Chemical Engineering
Chalmers University of Technology
SE-412 96 Gothenburg
Sweden
Telephone: +46 (0) 31 772 1000

DEM Modeling of Snow-Wall Adhesion

Development of a particle stick or bounce regime map for prediction of snow accumulation on cars

ANDERS LIND
Department of Chemistry and Chemical Engineering
Chalmers University of Technology, Gothenburg, Sweden

Abstract

A DEM model for particle-wall interaction was created for characteristics of dry snow. The snow properties used were partly obtained from a field test in northern Sweden at conditions of -20 °C and low humidity. Remaining physical properties were gathered from previous studies during the literature review. Implementation of the most reasonable contact model, the JKR model, was made to account for particle adhesion. The DEM model with the required input data was then used for development of a regime map for particle stick and bounce. Parameterization included normal velocity and particle diameter, and combinations of relevant values were used to span the regime map.

A sensitivity analysis was performed which showed that, within the significant ranges, the work of adhesion as well as the coefficient of restitution had the biggest impact on the collisional outcome. However, the method to estimate these two parameters was considered unreliable. It was found feasible to use the regime map for simulation of snow adhesion with CFD. Wind tunnel experiments were performed with a reference object to study the snow build-up. From comparison between the wind tunnel experiments and the CFD simulations the critical normal velocity for sticking was found to be of reasonable magnitude. To describe snow adhesion, additional parameters are required such as the tangential velocity and the shear stress. With the developed framework it is possible to use other parameterizations, while a two variable regime map is most suitable for implementation in a CFD model.

Keywords: Discrete Element Method, Snow, Regime map, Adhesion, Computational Fluid Dynamics

Acknowledgements

First of all, thanks to my examiner Professor Anders Rasmuson for helpful guidance and for entrusting me with this master's thesis. I would also like to really thank my supervisors PhD Per Abrahamsson and PhD Matthias Eng for superb supervision and for many interesting discussions throughout the thesis.

Further I would like to express my gratitude to my dear friend Markus Enmark for helping me during my thesis and for providing an inspiring working atmosphere. Thanks also to Mohammadreza Tamadondar and PhD Mohammad Khalilitehrani for your assistance and for keeping your doors open.

My colleagues at the division of Chemical Engineering at Chalmers as well as at Contamination and Core CFD at Volvo Cars all deserve my gratitude for their friendliness. Thank you especially to my fellow master's thesis students for motivating me and for making the time at Chalmers very enjoyable.

Last but certainly not least, thank you Hanna Blinge for believing in me and for helping me throughout the thesis and my entire studies at Chalmers.

List of abbreviations

VCC	Volvo Car Corporation
CFD	Computational Fluid Dynamics
Chalmers	Chalmers University of Technology
DEM	Discrete Element Method
JKR	Johnson, Kendall and Roberts
Fluent	ANSYS Fluent
COR	Coefficient Of Restitution
RANS	Reynolds Averaged Navier Stokes
DDES	Delayed Detached Eddy Simulation
LES	Large Eddy Simulation
PSD	Particle Size Distribution
UDF	User-Defined Function

Table of Contents

Abstract III
Acknowledgements IV
List of abbreviations V
1. Introduction 1
1.1 Background 1
1.2 Purpose 3
1.3 Limitations 4
2. Theoretical background 5
2.1 Formation and structure of snow particles 5
2.2 Discrete Element Method 6
2.3 Contact mechanics in particle collisions 8
2.3.1 Hertz theory 9
2.3.2 JKR theory 11
2.4 Computational Fluid Dynamics 12
3. Methodology 14
3.1 Particle properties from field studies 14
3.2 Particle properties from literature 15
3.3 DEM model 17
3.3.1 Implementation of contact mechanics 17
3.3.2 Modeling of collision with a flat wall 18
3.3.3 Modeling of collision with a rough wall 18
3.3.4 Sensitivity analysis of particle properties 19
3.4 Post-processing of DEM model 19
3.5 VCC climatic wind tunnel 19
3.5.1 Reference object 20
3.5.2 Snow adhesion test 20
3.5.3 Increased temperature and humidity test 20
4. Results 21
4.1 DEM input data 21
4.2 Regime map for particle stick or bounce 22
4.3 Sensitivity analysis of particle properties 23
4.4 Rough wall model 25

4.5 Validation of the DEM model....26
4.5.1 Use of regime map in CFD simulations....26
4.5.2 Comparison of wind tunnel experiments and CFD simulations....27
5. Discussion....29
5.1 Particle properties....29
5.2 Shortcomings of the DEM model....29
5.3 Parameterization of regime map....30
5.4 Modification of DEM model for other snow types....31
5.5 Suggestions for further work....31
6. Conclusions....32
References....33
Appendix A....36
Appendix A.1....36
Appendix A.2....36
Appendix B....38

1. Introduction

There are several incentives for the development of the autonomous driving car industry. Reducing the number of accidents, preventing congestion in traffic, and lowering the overall CO_2 emissions produced by cars are some of many benefits this technology could bring to our society (Thompson, 2016). Research and development within this area is currently performed by many companies and organizations, including Volvo Car Corporation (VCC). The autonomous driving technology in a Volvo car requires advanced equipment on the exterior of the car. For instance, numerous cameras, radars, sensors, and a laser scanner are needed (Volvo Car Corporation, 2016).

For safe and reliable operation of an autonomous driving vehicle, it is critical that the surface of the equipment is not blocked. On gravel roads or in extreme weather conditions, contamination from dust, rain, and snow can impair the optical access of the equipment on the exterior of the car (Eng, et al., 2017). Packed snow on the rear lights of the car is another problem that creates safety issues in the traffic. It is important to understand and predict accumulation of contaminants on the exterior of the car in order to make good decisions where sensitive equipment should be placed. Besides in field testing with existing cars, computer models such as Computational Fluid Dynamics (CFD) are very useful. They can be used as an efficient method to replace, or complement, real life tests both for existing cars and for models under development. Multiphase CFD models can be used for simulation of for instance contamination, where particles are suspended in an air flow.

Accumulation of snow is particularly challenging to predict due to its alternating and unknown properties. To develop a CFD model for this purpose, VCC is conducting a research project in cooperation with the division of Chemical Engineering at Chalmers. At the current stage, there is no method available to accurately predict where on the exterior of the car snow particles stick and where they bounce off. Many parameters may affect whether the collision results in stick or bounce, e.g. the adhesion force of snow and the impact velocity of the particle. Shear forces from the wind might also be a determining factor due to the rip off effect of snow accumulated on the surface of the car. The focus of this thesis, which is a part of the research project, is to investigate which parameters that are the most significant for snow adhesion by setting up a detailed collision model that can resolve the important physics of snow-car collision.

1.1 Background

There are several modeling approaches available to study the interaction between snow particles and the exterior of the car. Two commonly used models are the hard sphere model and the soft sphere model (Crowe, et al., 2012). These models use a rigid particle approach, meaning that no deformation of the particle geometry is considered. Both models are used solely for spherical particles, and the hard sphere model represents a less computationally heavy approach. This model calculates the post collisional velocity components directly using coefficients that predetermine the velocity change in the normal and tangential directions (Kosinski & Hoffmann, 2011). This model can, however, only account for binary collisions and particle flows with negligible impact from adhesive forces (Marshall & Shuiqing, 2014). Kosinski & Hoffmann (2011) explains that in the more advanced model, the soft sphere model, calculation of particle velocities and forces are performed using numerical integration of the equations of motion. This increases the computational effort

significantly. The soft sphere model is often shortened DEM which stands for the Discrete Element Method. The DEM model has a broader area of use since it is possible to implement physical phenomena more readily, e.g. cohesion and adhesion that are present in many types of particle flows (Kosinski & Hoffmann, 2011).

Another common approach is to use the Finite Discrete Element Method, which takes particle deformation into account. However, for most cases the DEM model represents a more favorable tradeoff between accuracy and computational effort. Numerical modeling using DEM is therefore important in many fields, for instance in the pharmaceutical and food industries (Bertrand, et al., 2005). The model was initially formulated by Cundall & Strack (1979) and it was intended for nonadhesive contacts of granular flows. This model is sufficient for cases with relatively large particles, where gravity and particle inertia govern the dynamics. For systems with particles in the micro scale on the other hand, attractive forces become important. Fortunately, progress has been made of how to modify and extend the contact models to include adhesion and intermolecular forces (Marshall & Shuiqing, 2014).

Modeling of adhesive particle flows using DEM has thoroughly been studied and performed by Li et al. (2011). The paper reviews agglomeration, i.e. formation of particle assemblies kept together by weak adhesive forces, and also the dominant contact forces present in such systems which includes van der Waals forces, ligand-receptor binding, liquid bridging forces, interfacial attractive forces, and sintering forces. Nguyen et al. (2014) also studied agglomerates and examined collision between a particle and an agglomerate to create a regime map of the collisional behavior using DEM. In this study, the contact model that is known as the Johnson, Kendall and Roberts (JKR) theory was used to simulate the attractive forces originating from adhesion of the particles. The JKR model was developed back in 1971 by Johnson et al. as a modification of the Hertz equation which models collision and contact of spherical particles without adhesion.

When it comes to modeling of snow the vast majority of the research has been conducted in geophysics, with dedication specifically to avalanches. To be able to perform controlled experiments for this purpose, Steinkogler et al. (2015) used a tumbler to investigate granulation of snow and its temperature dependence. The granulation equipment was then set up with a DEM model in order to reproduce the experiments. It was concluded that above -1 °C, where more liquid water is present on the particle surfaces, agglomeration showed a rapid increase due to greater forces of cohesion (Steinkogler, et al., 2015). On the smaller scale, i.e. for individual particles, numerous studies have been made with focus towards ice particles present in planetary rings (Higa, et al., 1998) (Hatzes, et al., 1988). The contact behavior has been studied and has shown that is greatly affected by temperature as well as the presence of frost on the particle surfaces.

To perform simulations of snow particles and a driving car, VCC is using a multiphase Euler-Lagrangian model in the CFD software ANSYS Fluent. The air flow is modeled as the continuous phase while the snow particles, which are injected around the surface of the tires, are modeled as the discrete phase. To model collision between particles and a wall, different boundary conditions are used depending on the characteristics of the discrete phase particles. The most relevant discrete phase boundary conditions available within the ANSYS Fluent framework are reflect, trap, and escape (Fluent User's Guide, Release 17.0). A more complex boundary condition is required for simulation

with snow particles however, since many parameters and physical properties decide whether particles stick or bounce at collision with a surface.

To gain knowledge about contamination and properties of snow, field studies and tests have been performed by VCC and Chalmers earlier in the overall research project. A comprehensive field study was made during winter in the north of Sweden to investigate snow build-up on cars driving on a snowy road (Eng, et al., 2017). The study was also made to determine the structure and properties of snow particles (Abrahamsson, et al., 2017). The snow particles were dry, i.e. no liquid water was present on the surfaces, due to a temperature of about -20 °C and low humidity. VCC focuses on CFD simulations of vehicle self-contamination, which refers to snow lifted up by the tires of the vehicle itself (Gaylard, et al., 2014). Therefore, snow aged on the ground was investigated. Particles that accumulated on cars were deemed to be spherical based on the field studies made prior to the thesis (Abrahamsson, et al., 2017) (Eng, et al., 2017). Size distributions of snow particles were also found using a microscope.

In the field test in northern Sweden the adhesion properties were measured for snow particles (Abrahamsson, et al., 2017). Since one of the more contamination sensitive equipment, the radar, has plastic covers, snow-plastic adhesion was measured. Adhesion between snow and other materials was also investigated and the difference was deemed insignificant. Properties of other snow types have also been investigated including wet snow from Göteborg, snow from Volvo climatic wind tunnel, and snow artificially produced in a laboratory. These properties and their effect on the choice of contact model in a DEM model will be discussed, while characteristics of dry snow were used in the DEM model in the thesis.

1.2 Purpose

Developing a DEM model that correctly describes the mechanics of snow particle collisions is an essential part of this project. This includes implementation of the most relevant contact models and finding as correct physical properties of snow as possible. A sensitivity analysis of important parameters will be made to determine their impact on the result. Further the DEM model will be used to create a regime map of particle stick and bounce by finding the most relevant parameterization. The regime map will be used in the development of a method to predict snow accumulation within the CFD software Fluent. An important remark is that the work within Fluent is not a part of this thesis, but is performed in a parallel master's thesis (Enmark, 2017). Validation of the DEM model will be performed by comparison of the CFD simulations with field and wind tunnel tests.

The most important questions that the thesis aims to answer are:

- Which contact models should be used for snow particle-wall interaction?
- What parameters are most suitable for parameterization of a regime map for particle stick and bounce?
- Which parameters affect the results from the DEM model the most?
- Can the DEM model, with some degree of modification, be used for different types of snow?
- Can the DEM model provide a physically reasonable interpretation of snow adhesion?
- Are some important phenomena left out in the model?
- How can the model be validated using experimental trials?

1.3 Limitations

The structure of the snow particles used in the DEM model will be regarded as perfectly spherical. No impurities will be considered and completely smooth particle surfaces will be assumed for the model. The exterior of a car consists of several materials, but in the DEM model the wall properties will be that of plastic. For validation of the model, a reference object will be used in wind tunnel tests and CFD simulations. This simplified object will reduce the computational time required for the simulations in the developing stage of the model.

2. Theoretical background

The characteristics of snow, in terms of its structure and physical properties, alter significantly depending on the ambient temperature and humidity. Another factor that comes in to play is the age of snow, i.e. the time of its deposition on the ground. The theoretical background will start with giving the required knowledge about the characteristics of snow, mainly dry snow (no liquid water on the particle surfaces) which is used in the DEM model in the thesis. The theory about DEM will then be explained before moving on to the most relevant contact models, and finally this chapter will give a basic understanding about the CFD model used by VCC for simulation of particles and a driving car.

2.1 Formation and structure of snow particles

Snow is a complex granular material that has a wide range of structures. It originates from the atmosphere when deposition of water vapor into ice initiates the formation of snow crystals. The deposition of water vapor requires a nucleus, which in the air is present in the form of dust particles (Libbrecht, 2007). The angle between bonds of atoms in a water molecule promotes an initial growth of a hexagonal lattice structure. As the deposition of water vapor progresses onto the formed hexagonal ice lattice, it continues to grow and various types of snow crystal structures have been found (Libbrecht, 2007). To understand the complexity of snow crystals, Japanese physicist Ukichiro Nakaya grew crystals artificially in laboratory experiments (Nakaya, 1954). He discovered that the crystal growth was strongly dependent on the temperature as well as the humidity of the air. Nakaya's work laid the foundation for development of a morphology diagram for snow crystals that explains how they grow at different temperatures and humidities (Figure 1).

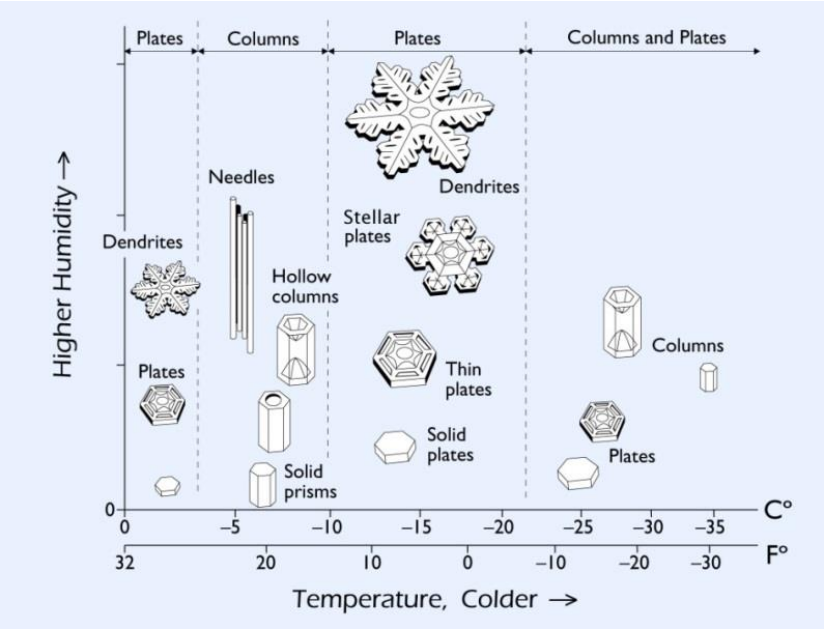

Figure 1. Metamorphism of snow crystals for common air temperatures and humidities (Libbrecht, 2016).

The snow crystals grow larger gradually and eventually gravity governs the movement of the particles. Alongside crystal growth, snowflakes are formed when agglomeration occurs as crystals collide with each other. When snow particles settle on the ground the microstructure continues to

change as metamorphism take place (Miller, et al., 2003). The phenomenon of metamorphism differs significantly depending on the amount of liquid water present in the snow. It is therefore common practice to divide the process into two categories, one for wet snow and one for dry snow (Colbeck, 1986). The metamorphism is not only dependent on how much water that is present in the snow layer, but also on the temperature gradient in the snow layer. Dry snow either experiences equilibrium metamorphism, when there is a low temperature gradient in a snowpack, or kinetic growth metamorphism, which occurs when the temperature difference is large (Miller, et al., 2003).

Without a temperature gradient, no phase change of snow particles can take place since it requires a heat flow. The growth rate of particle clusters rapidly increases with increasing temperature difference. For dry snow, Colbeck (1986) and Miller et al. (2003) state that equilibrium metamorphism generally gives rise to rounded particles whereas kinetic growth metamorphism forms faceted particles. However, since the temperature gradient often varies in a snow pack, there are many possible paths for growth of rounded and faceted crystals. Other factors also affect the growth rate, such as the density of the snow (Colbeck, 1986). Figure 2 visualizes the metamorphism in a snow layer with temperature gradient over time.

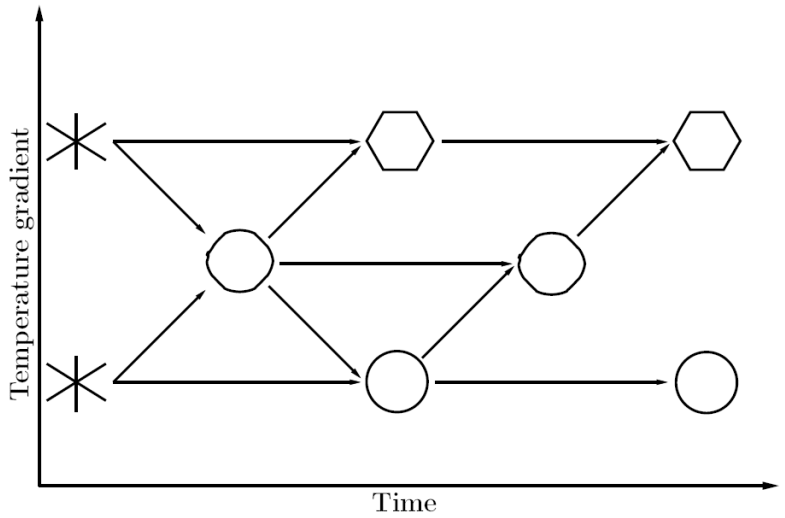

Figure 2. The snow metamorphism in a snow layer as a function of temperature gradient and time. Small temperature differences (equilibrium metamorphism) form rounded particles and large temperature differences (kinetic growth metamorphism) form faceted particles. Intermediate temperature difference may form more complex structures.

2.2 Discrete Element Method

When a particle collides with a wall or with another particle, a force is exerted between the two solid bodies and as a result deformation takes place. Rigorous computation of deformation of particles is time consuming and simplification is needed for practical applicability (Crowe, et al., 2012). Cundall & Strack (1979) developed a method that simplifies the modeling for discs and spheres. This method is called the soft sphere model and is more commonly known as the DEM model for its use in computer simulations (Crowe, et al., 2012). It models particles as individual entities using force balances for their movement and collisions, and it is based on Newton's second law of motion (Jin, et al., 2011). Instead of accounting for particle deformation, the DEM model uses an overlap between colliding particles. The overlap is created due to the force exerted between the bodies, and it generates a repulsive force that increases with the size of the overlap. The main sequence of events for a collision between a particle and a wall with DEM can be illustrated according to Figure 3.

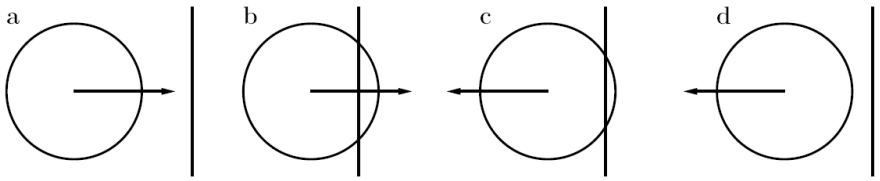

Figure 3. Stages of a particle collision with arrows showing the direction of the particle movement. a) The particle is approaching the wall. b) The maximum overlap is reached as the particle velocity is dampened and reaches zero. c) The particle is repulsed from the wall. d) The particle is leaving the wall.

The idea of using an overlap instead of particle deformation is explained in the original work by Cundall & Strack (1979). They state that compared to larger assemblies in a granular flow, such as agglomerates, the deformation of a single particle is small. Further, the overlap created in a particle collision is small compared to the size of the particle (Cundall & Strack, 1979). The repulsive force generated from the overlap is modeled according to a spring. As the spring is compressed, a repulsive force arises. Modeling of a particle collision with a spring symbolizes a fully elastic system with no loss of kinetic energy. In reality though, dissipation of energy occur by different physical phenomena such as viscoelasticity at low impact velocities and plastic deformation at high impact velocities (Krijt, et al., 2013). This is taken into account by introduction of a dashpot as a mechanical component to model loss of kinetic energy (Crowe, et al., 2012). A dashpot (viscous damper) absorbs energy and the combined system is illustrated in Figure 4, while Equation (1) gives the differential form for the motion of a particle with mass m.

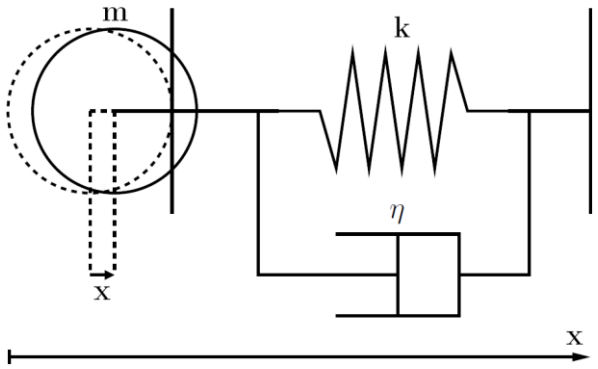

Figure 4. Spring-dashpot system that is used in the soft sphere model for collision of a spherical particle. The dotted circle represents a particle in the equilibrium state in contact with a wall. The solid circle represents a particle during collision with the wall. The spring produces a repulsive force that increases with the size of the overlap, and energy dissipation is modeled with the dashpot component.

$$m\ddot{x} + \eta\dot{x} + kx = 0 \tag{1}$$

In Equation (1) m is the particle mass, η is the damping coefficient of the dashpot, k is the stiffness coefficient of the spring, and x is the distance from the particle center to the equilibrium position which is the same as the size of the overlap. Computation using the spring-dashpot model is performed when a particle collides with a wall or another particle. The kinetic energy that is absorbed by the dashpot reduces the magnitude of the post collisional particle velocity as it returns to the equilibrium position. The amount of kinetic energy lost in a collision is often regarded as a material property and is described with the coefficient of restitution (COR) (Krijt, et al., 2013). COR, often denoted as e, is the ratio of the relative velocities post and pre collision, v_p and v_i, according to Equation (2). Crowe et al. (2012) explains that the damping coefficient, η, of the dashpot in Equation (1) can be related to e. The result is shown in Equation (3).

$$e = \left| \frac{v_p}{v_i} \right| \tag{2}$$

$$\eta = -\frac{2 \ln e}{\sqrt{\pi^2 + \ln e}} \sqrt{mk} \tag{3}$$

The most basic case for a particle collision is when the direction is normal towards a surface. However, a moving particle will most likely have both normal and tangential velocity components, leading to an oblique impact (Crowe, et al., 2012). In an oblique impact, friction between the particle and the wall has to be considered. If the force in the tangential direction is greater than the limit of the Coulomb criterion of friction, as shown in Equation (4), sliding during collision will occur and a tangential overlap will arise. This overlap is modeled separately from the normal overlap, with a spring-dashpot system in the tangential direction (Crowe, et al., 2012). The frictional force that dampens the kinetic energy in the tangential direction is limited by the Coulomb criterion and the force is calculated by the spring-dashpot system. The coefficient of friction μ in Equation (4) is a property between two materials. It describes the ratio between the maximum frictional force F_f in a static contact and the normal force F_n applied between the materials.

$$F_f \leq \mu F_n \tag{4}$$

To resolve the mechanics of a particle collision, the differential form of Newton's second law of motion is solved by numerical integration with an appropriate time step. The time scale for which a particle collision occurs is usually very small, especially for rigid materials. This leads to an inherent numerical stiffness for DEM computations (Marshall & Shuiqing, 2014). The time step required for a simulation depends on the model that is used. The most elemental model is the linear spring-dashpot system described by Equation (1). However, for many material types the particle interactions are not well described by a linear force displacement relation (Crowe, et al., 2012). A non-linear contact model, e.g. the Hertzian contact theory, is therefore commonly used instead (Thornton, 2015). There are also various contact models that can be implemented for adhesive interaction in a DEM model, and the choice depends on the characteristics of the particle and target materials. This will be further discussed in the next section.

2.3 Contact mechanics in particle collisions

Different mechanisms for dissipation of energy take place in particle collisions. The particle size, the properties of the particle and target material, and the impact velocity affect the magnitude of the energy dissipation. If the dissipation of energy is in the same order of magnitude as the pre collisional kinetic energy, the collision could result in sticking of the particle. This is typically the case for low impact velocities, whereas collisions with high impact velocity generally lead to particle bounce (Krijt, et al., 2013). Simulation of particle interaction is performed to calculate the contact force and decide whether the outcome is stick or bounce. Contact models are available for non-adhesive interaction, and also for interactions where adhesive forces are present.

The mechanics and force of contact can be modeled through various methods. For non-adhesive particles, the mechanics boils down to elastic and elastic-plastic interaction (Thornton, 2015). If no force is applied in a particle-particle or particle-wall interaction, the contact only take place in a single point called the contact point. An applied force will cause particle deformation, and in DEM elastic deformation is modeled as an overlap. The force acting in a contact between two non-

adhesive elastic spheres was predicted in the Hertz theory (Hertz, 1882). In this theory the deformation gives rise to a contact area with the shape of a circle with radius a_h, according to Figure 5 (Marshall & Shuiqing, 2014). In systems with particle diameters at or below the micrometer scale however, adhesion becomes important for particle-particle and particle-wall interactions (Li, et al., 2011). Different theories have therefore been developed to modify the Hertzian pressure distribution to account for the effect of adhesion forces in the contact mechanics.

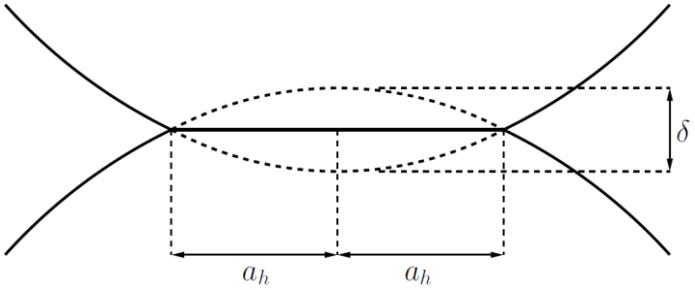

Figure 5. Contact between two spherical particles with mutual approach δ. The deformation creates a circular contact area with radius a_h.

The two most common adhesive contact models for van der Waals forces are the JKR model and the DMT model. In the JKR model the assumption is made that a contact area arises due to elastic deformation, while the DMT model assumes that the particles remain spherical during contact (Marshall & Shuiqing, 2014). The general agreement is that for relatively large particles the JKR theory applies, while the DMT model is mostly used on the molecular scale (Thornton, 2015). When water is present, liquid bridging between particles occur which is a much stronger adhesive force compared to van der Waals forces. This force is relevant for particle diameters up to the magnitude of millimeter, and requires a separate contact model compared to cases with dry particles (Li, et al., 2011).

2.3.1 Hertz theory

For non-adhesive elastic spheres, Hertz (1882) proposed a theory for calculation of the contact force. The theory uses a non-linear relation, unlike the one shown in Equation (1), and describes the normal force with the normal displacement (overlap) to the power of 3/2 (Crowe, et al., 2012). A requirement for the validity of the theory is that the contact area radius, see Figure 5, is small in comparison to the radii of the particles in contact. In the work of Krijt et al. (2013), the derivation of the Hertzian elastic contact theory is summarized for the normal direction. For the contact area a_h, the pressure distribution for two elastic spherical particles can be written as:

$$p(r) = \frac{E^*}{\pi R^*} \frac{a_h^2 - 2r^2 + R^*\delta}{\sqrt{a_h^2 - r^2}} \tag{5}$$

For particle-particle contact of two identical spheres, the mutual approach δ is the summation of both overlaps (Figure 5). For particle-wall contact the mutual approach is the overlap of the particle, while the wall is regarded as a sphere with infinite radius. E^* in Equation (5) combines the Poisson's ratio and Young's modulus of the particles to the combined elastic modulus which is defined as:

$$\frac{1}{E^*} = \frac{1 - \nu_1^2}{E_1} + \frac{1 - \nu_2^2}{E_2} \tag{6}$$

The Poisson's ratio, ν_i, and the Young's modulus , E_i, are material properties of the particles. The Poisson's ratio, which describes the directional magnitude in which a material expands due to compression, is the ratio of transversal expansion and axial compression. The Young's modulus describes the stiffness in elastic materials as the ratio between tensile stress and extensional strain. Finally, R^* in Equation (5) is the relative surface curvature for contact between particles with radii R_1 and R_2 and is defined as:

$$\frac{1}{R^*} = \frac{1}{R_1} + \frac{1}{R_2} \tag{7}$$

The pressure distribution, given by Equation (5) for contact radius $0 \leq r \leq a$, reaches the maximum compressive stress when $r = 0$, and the total normal elastic force is defined as:

$$F_{ne} = \int_0^a p(r) 2\pi r dr = \frac{2E^*}{3R^*}\left(3a_h \delta R^* - a_h^3\right) \tag{8}$$

The contact of the particles stores energy by elastic strain according to:

$$U_{ne} = \frac{E^* a_h^3}{3R^*}\left(\delta\left(\frac{3\delta R^*}{a_h^2} - 1\right) - \frac{a_h^2}{5R^*}\left(\frac{5\delta R^*}{a_h^2} - 3\right)\right) \tag{9}$$

The equilibrium contact area is found when the elastic strain energy is minimized, i.e.:

$$a_h^2 = R^* \delta \tag{10}$$

Inserting Equation (10) into Equation (8) and rearranging gives the classical expression of the Hertzian force for elastic contact (Krijt, et al., 2013) (Marshall & Shuiqing, 2014) (Thornton, 2015):

$$F_{ne} = \frac{4E^* a_h^3}{3R^*} \tag{11}$$

The stiffness coefficient of the spring for the Hertzian contact theory is, for two identical particles with radii $R_i = R_j$, expressed as a function of their physical properties (Crowe, et al., 2012):

$$k_n = \frac{\sqrt{2R}E}{3(1-\nu^2)} \tag{12}$$

With the stiffness coefficient k_n, the particle mass m, the normal displacement δ_n, and a coefficient α that is related to the COR, the damping coefficient can be expressed as (Crowe, et al., 2012):

$$\eta_n = \alpha\sqrt{m k_n}\delta_n^{\frac{1}{4}} \tag{13}$$

With the stiffness predicted by the Hertz theory, the time step required for numerical integration can be related to the oscillation period of the system. The oscillation period can be calculated using Equation (14) and the time step should be one magnitude smaller than the calculated time period.

$$\Delta t = 2\pi\sqrt{\frac{m}{k_n}} \tag{14}$$

2.3.2 JKR theory

When a particle comes into contact with another particle or a wall, adhesion by means of van der Waals forces arise between the solid surfaces from molecular interaction (Crowe, et al., 2012). Johnson, Kendall, and Roberts (1971) investigated adhesion between elastic spheres and proposed a model based on the contact radius given by the Hertz theory (Johnson, et al., 1971). An assumption made in the model, known as the JKR model, is that the length scale of the van der Waals forces is several order of magnitudes smaller compared to the elastic deformation. Tabor (1977) proposed a parameter that compares the length scales of van der Waals forces and the elastic deformation (Tabor, 1977). The parameter is defined according to Equation 15, where Γ is the work of adhesion and z_0 is the separation of molecules.

$$\lambda_T = \left(\frac{R^*\Gamma^2}{E^{*2}z_0^3}\right)^{1/3} \tag{15}$$

In the JKR model the contact area for adhesive interaction is slightly larger than the Hertzian contact area in Figure 5 ($a > a_h$). This is a result of a surface energy term that is added to the total energy of the system (Krijt, et al., 2013). The contact area for adhesive particle-particle or particle-wall interaction can be written as a function of the elastic contact force in the normal direction according to (Marshall & Shuiqing, 2014):

$$a^3 = \frac{3R^*}{4E^*}\left(F_{ne} + 3\pi R^*\Gamma + \sqrt{6\pi R^*\Gamma F_{ne} + (3\pi R^*\Gamma)^2}\right) \tag{16}$$

In Equation (16) Γ is the work of adhesion for particle interaction. An equilibrium state for particles in contact is obtained when the normal elastic force F_{ne} equals zero. In that state there is a balance between adhesive attraction and elastic repulsion, and the equilibrium contact area radius is obtained from Equation (16) by inserting $F_{ne} = 0$:

$$a_0 = \left(\frac{9\pi\Gamma R^{*2}}{2E^*}\right)^{1/3} \tag{17}$$

For a sticking collision of a particle, the area for the particle contact at equilibrium is hence given by Equation (17). To break the particle interaction a pull-off force is required, often denoted as the critical force F_c which is equal to:

$$F_c = \frac{3\pi\Gamma R^*}{2} \tag{18}$$

A phenomenon known as necking occurs when a force is acting to break an adhesive particle contact. This means that the contact remains active, even when no overlap exists, until the pull-off force is reached. This is described by Thornton (2015) and the compression and recovery stages of a particle collision can be illustrated according to Figure 6 where the contact area α is plotted against the normal elastic force F_{ne}. When a particle-particle or particle-wall contact is made an attractive force arises from adhesion and F_{ne} drops to point A. During compression, the repulsive force increases the magnitude of F_{ne} until the maximum contact area is reached at point B. During the recovery stage

the contact does not break at point A where the contact area reaches zero. Instead the contact breaks at point C when the critical force F_c, given by Equation (18), is reached. Complete separation occurs at point D, where there is a negative overlap that gives rise to a contact area of size α_f which can be described by Equation (19).

$$\alpha_f = \left(\frac{3F_c^2}{16R^*E^{*2}}\right)^{\frac{1}{3}} \tag{19}$$

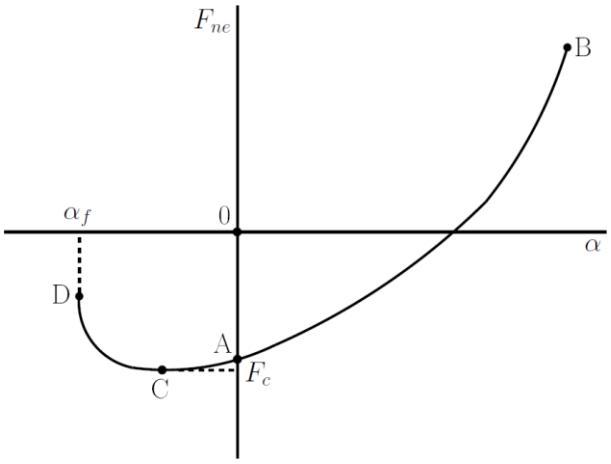

Figure 6. The compression and recovery paths for an elastic-adhesive particle interaction explained with a relation of the normal elastic contact force and the contact area. The loading stage starts at point A when a contact is made, B is the point of maximum compression, C is where the contact breaks, and D is where complete separation occurs.

2.4 Computational Fluid Dynamics

Simulation in CFD of a fluid flow and solid particles is performed using a multiphase model. The most common multiphase model for granular flows is the Euler-Lagrange model. VCC is using the Euler-Lagrange model in the project, with the air flow solved in the Eulerian framework as the continuous phase with turbulence models further described down below. The particles are modeled with the Lagrangian framework as the discrete phase and the particle trajectories are found by solving their force balances (Eng, et al., 2017).

The Euler-Lagrangian framework works well for both one and two-way coupling, which is characterized by the Stokes number. Stokes number compares the timescales of the discrete phase and the continuous phase, providing a measure to which extent the phases affect one another (Andersson, et al., 2014). The case with snow particles in a turbulent air flow has a low Stokes number. This means that the particles follow the air flow since their movements are governed by the aerodynamic drag and not by inertia (Eng, et al., 2017). In a dilute dispersed flow of snow particles the continuous phase is unaffected by the discrete phase, hence it is possible for a steady-state case to solve the flow field initially and resolve particle tracking as a post-processing step (Andersson, et al., 2014). In a dense flow the particle-particle collisions governs the particle movements. To differentiate between a dilute and a dense flow the magnitudes of the momentum response time and the average time between particle-particle collisions can be compared (Crowe, et al., 2012). Normally the computational effort for tracking of individual particles is excessive. The particles are therefore divided into parcels in the simulations. Each parcel is tracked as an individual particle but carries a number of particles (Fluent Theory Guide, Release 17.0).

In the project, VCC has performed steady-state simulations of a car with snow particle injection. This was performed by using a k-ε turbulence model that solves the Reynolds Averaged Navier Stokes (RANS) equations for the air flow, and to account for turbulent fluctuations a particle dispersion model was used (Eng, et al., 2017). The results have shown that this model, compared to real life experiments, has not been able to successfully predict the particle distribution on the car. A more accurate turbulence model in transient simulations has therefore been used instead to capture the unsteady flow structures of the air flow. The model that is used is the Delayed-Detached Eddy Simulation (DDES) model (Eng, et al., 2017). Unsteady simulation with this model solves the RANS equations in the boundary layer close to the wall if the grid is fine enough; otherwise Large Eddy Simulation (LES) is performed. In the bulk air flow the large scale eddies are solved while the small turbulent scales are accounted for implicitly by the use of a subgrid model (Fluent Theory Guide, Release 17.0). The model is described in more detail by Sterken et al. (2016).

As particles are brought into contact with a surface, the boundary condition used decides the outcome of the collisions. Particles with very high kinetic energy, such as small stones from a gravel road, bounces on impact with a surface and the reflect boundary condition is used in that case. For small adhesive particles the trap boundary condition can be of relevance in some situations. Another common case is water droplets that absorb into a liquid film upon collision, which the wall-film boundary condition is suitable for (Eng, et al., 2017). For particles that require a more complex impingement condition, such as snow particles, it is possible to model the impact behavior by implementation of user-defined functions (Fluent User's Guide, Release 17.0). This method will be used in the parallel master's thesis by Enmark (2017), where information from the DEM model will be used to create a boundary condition.

3. Methodology

As the first step of the thesis work, a literature review was made on snow characteristics, DEM modeling, and CFD. The review about snow characteristics was focused on understanding particle structures and how they form, and even more importantly on finding the required particle properties for the DEM model. From the field study in northern Sweden performed prior to this thesis, the particle size distribution (PSD) and force of adhesion for dry snow particles were determined. Remaining properties required for the DEM model were found in literature or derived analytically.

The literature review on DEM modeling was made to get a basic understanding of important theory and to learn about related studies within that area. The software used in the thesis for the DEM model will be introduced in a subsection to this chapter. The choice of contact model will be described and the methodology behind the choice will be presented. The approach of developing a regime map for particle stick and bounce will then be described, both how the DEM model was set up and how post-processing was executed. Finally, this chapter will describe the experimental tests made in this thesis to enable validation of the DEM model and the regime map created in this thesis.

3.1 Particle properties from field studies

From the field study in northern Sweden it was concluded that the particles that accumulated on cars could be deemed as spherical. This suggests that equilibrium metamorphism took place during the aging of the snow, which formed rounded particles. Based on that conclusion, a perfectly spherical snow particle structure was assumed which basically correspond to a solid ice particle; hence the density of ice was assumed for the particles. Common impurities in snow includes soluble materials and particles of soot, dust and sand (Fierz, et al., 2009). For simplification in this thesis it was assumed that the particles had no impurities. As for the PSD, a noticeable difference was found between snow particles from the ground, and the snow particles that accumulated on the rear surface of a car. Figure 7 and Figure 8 shows a comparison of the PSDs and the trend was that particles that accumulate on the rear side of a car was generally very small compared to the range of diameter sizes found on the ground. Since the focus of the thesis was snow accumulation, a size range of 0.01-0.1 on a normalized scale was chosen from the PSD in Figure 8.

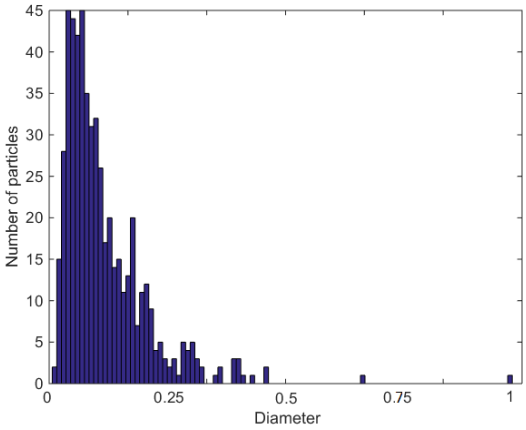

Figure 7. Normalized PSD for snow on the ground.

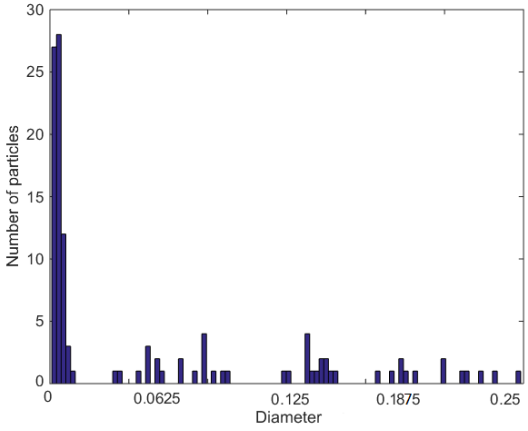

Figure 8. Normalized PSD for snow accumulated on the rear surface of a car.

In addition to the particle structure and size distribution, the adhesion force for snow-wall interaction was measured by Abrahamsson et al. (2017). A load cell was used that creates an electrical signal with a magnitude proportional to the force acting on the load cell. Snow agglomerates were placed on the load cell and pressed against a wall multiple times while the force was measured continuously (Figure 9). The measured force was then used to calculate the work of adhesion, Γ, which was derived using correlations proposed by Thornton (2015). In Appendix A.1 the full calculation for the work of adhesion is presented. The work of adhesion for dry snow from northern Sweden was found to be within a range of 0.1 and 1 J/m^2, with an average of 0.2 J/m^2. Properties for other snow types were investigated by Abrahamsson et al., including wet snow from Göteborg, artificially produced snow from laboratory, and snow from the climatic wind tunnel at VCC. In the DEM model however, the dry snow properties were used.

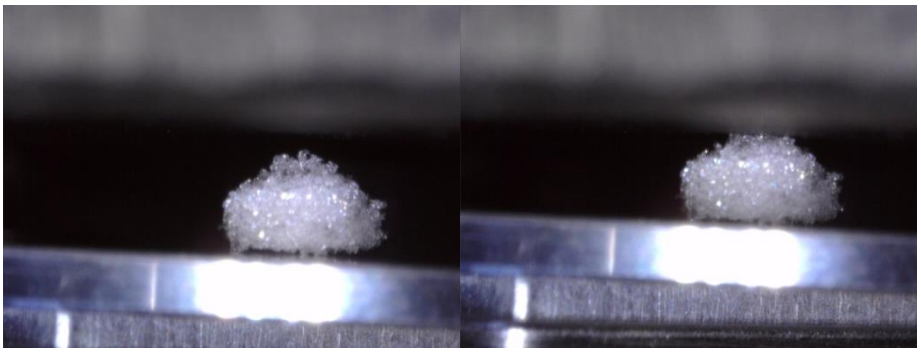

Figure 9. Images from the snow adhesion experiments where agglomerates were placed on a load cell while the force was measured. The agglomerate was pressed against a wall and pulled away from the wall multiple times.

3.2 Particle properties from literature

There are several mechanical properties that are required for DEM modeling of particles. For the Young's modulus and the Poisson's ratio the most relevant values found in literature are compiled in Table 1. Fletcher (1970) summarized elastic properties of ice, more specifically polycrystalline ice at -5 °C with grains in the millimeter to centimeter size range. Amongst other mechanical properties for the grains, the range of the Young's modulus and the Poisson's ratio were reported. Higa et al. (1998) performed experiments to study collisions of ice spheres. The radius of the spheres ranged between 0.14 and 3.6 cm, and the Young's modulus used in the experiments was derived as a function of the temperature:

$$E = \frac{100}{10.40(1 + 1.070 * 10^{-3}T + 1.87 * 10^{-6}T^3)} \quad (20)$$

In Equation (20), E is in GPa and the temperature is in °C. The majority of the experiments by Higa et al. (1998) were performed at a temperature of -12 °C. The Young's modulus for that temperature as well as the Poisson's ratio used are shown in Table 1. Petrovic (2003) reviewed mechanical properties for both ice and snow. Young's modulus and Poisson's ratio for polycrystalline ice plates at -10 °C with a diameter of 0.5 m were reported.

Table 1. Literature values of Young's modulus and Poisson's ratio for ice.

Literature source	Young's modulus [GPa]	Poisson's ratio [-]
Fletcher (1970)	**8.9-9.9**	**0.31-0.36**
Higa et al. (1998)	**9.8**	**0.31**
Petrovic (2003)	**9.7-11.2**	**0.29-0.32**

The coefficient of restitution (COR) is often considered a material property as a measure of the loss of kinetic energy at collision. An analytical derivation of the COR in the normal direction for adhesive elastic-plastic spheres was given by Thornton & Ning (1998). They assumed that the loss of kinetic energy due to plastic deformation and work of adhesion are additive (Thornton & Ning, 1998). The COR was defined as:

$$(1 - e_n^2) = \left(1 - e_p^2\right) + (1 - e_a^2) \tag{21}$$

In Equation (21), e_n is the total COR in normal direction, e_p is the COR for plastic deformation, and e_a is the COR for work of adhesion. The contribution to e_n due to adhesion can be modeled in DEM with the work of adhesion, which was estimated in the experiments made by Abrahamsson (2017). For normal impact of a particle considered to be elastic-perfectly plastic, the contribution due to plastic deformation was derived by Thornton (1997). He gave an equation of e_p as a function of the yield velocity, V_y, and the impact velocity, V_i. The yield velocity is the maximum relative velocity for a purely elastic collision, and above that velocity plastic deformation takes place. Appendix A.2 presents the derivation of the COR due to plastic deformation.

Mechanical properties of the wall material are also required for the DEM model. Experiments were conducted prior to this thesis to measure the adhesion force between a plastic material and snow. Plastic is used as the material for covers to radar equipment, and its properties were therefore used for the wall in the DEM model. A conventional plastic material (ABS) was used, and the properties for the wall and particles that were used as input data to the DEM model are summarized in Table 2. The properties of ice proposed by Higa et al. (1998) were used primarily in the DEM model because of the fact that the experiments were performed with ice spheres. Their experiments represent the spherical particles modeled in this thesis the best, although the length scale of the diameters was significantly larger. Extreme values found in other studies in literature, seen in Table 1 above, were used in a sensitivity analysis to examine which parameters that affected the results the most.

Table 2. Properties for ice particle and plastic wall for DEM model.

Property	Particle (ice)	Wall (plastic)
Density [kg/m^3]	**920**	**1100**[1]
Young's modulus [GPa]	**9.8**	**2.0**[1]
Poisson's ratio [-]	**0.31**	**0.35**[2]
Work of adhesion [J/m^2]	**0.2**	**0.2**

[1] (Cambridge University Engineering Department, 2003 Edition)
[2] (Professional Plastics, 2017)

3.3 DEM model

In order to simulate snow particle-wall collisions a DEM model was created. The model was built in the open-source software LIGGGHTS which is used for DEM particle simulations and also for CFD-DEM coupling (Kloss, et al., 2012). LIGGGHTS has previously been used for simulation in areas such as agglomerate collisions (Nguyen, et al., 2014) and snow particle modeling (Vedachalam, 2011). In the existing framework of LIGGGHTS there are several contact models available, and the source code can be modified and extended to include physics of a specific application. The input data to the DEM model was based on field and laboratory tests of snow particle properties, as well as properties found during the literature review on relevant studies previously performed.

3.3.1 Implementation of contact mechanics

For particle-particle and particle-wall interactions in LIGGGHTS the contact force is calculated when there is an overlap. The total contact force is expressed as:

$$F = (F_{ne} - F_{nd}) + (F_{te} - F_{td}) \tag{22}$$

In Equation (22), F_{ne} is the normal elastic force, F_{nd} is the normal damping force, F_{te} is the tangential elastic force, and F_{td} is the tangential damping force. In LIGGGHTS the Hooke model and the Hertz model are available for calculation of the contact force in particle collisions. The Hookean model provides a linear correlation between the force and the displacement, which generally is not considered to describe the physics appropriately as mentioned in the theoretical background. The Hertzian model, which uses the contact area to calculate the force non-linearly, provides a better approach for most particle-particle and particle-wall interactions.

To include adhesion by means of van der Waals forces, the LIGGGHTS framework provides a simplified version of the JKR model. It is valid for the Hertzian theory and the model adds a normal force that contributes to maintain particle contacts. However, an additive solution between the contact force from Hertz and from the simplified JKR is inaccurate. Implementation of the real JKR model, which was described in the theoretical background, has been done previously (Nguyen, et al., 2014). This was performed by modification of the existing Hertz model to account for the increasing contact area due to the attractive van der Waals forces that pull particles together.

To check if the JKR model was valid for the snow particle-plastic wall interaction, the Tabor parameter, see Equation (15), was evaluated. For a particle-wall case, R^* reduces to the particle radius since the wall can be considered as a sphere with infinite radius. Equation (6) was used to calculate the combined elastic modulus, E^*, with the properties of ice and ABS plastic from Table 2. Krijt et al. (2013) states that z_0, the spacing between atoms, is usually considered to be between 0.2-0.4 nm. Crowe et al. (2012) states that for the case of contact between two plates in air, the separation distance is the mean free path which for air molecules is equal to 0.4 nm. With these properties the Tabor parameter was calculated, see Equation (23), which was found to be in range of 9.6-41.3 depending on the particle size and the spacing between atoms. Since the Tabor parameter was above 5 for all cases, the JKR theory is valid (Krijt, et al., 2013) (Thornton, 2015).

$$\lambda_T = \left(\frac{R^* \Gamma^2}{E^{*2} z_0^3}\right)^{1/3} \rightarrow \; 9.6 \leq \lambda_T \leq 41.3 \tag{23}$$

3.3.2 Modeling of collision with a flat wall

To study the impact behavior of snow particles and a surface, a fundamental case with a single particle and a wall was set up and modeled with DEM. The model included a domain that contained a wall with properties of plastic, and a particle with properties of ice (due to the assumption of perfect sphericity). The size of the time step required for a DEM simulation can be estimated using the correlation for non-linear models provided by Equation (14). For the range of particle diameters considered in the model the size of the time step should be:

$$\Delta t = \frac{1}{10} 2\pi \sqrt{\frac{m}{k_n}} = \frac{\pi}{5} \sqrt{\frac{V\rho}{\frac{\sqrt{2R}E}{3(1-\nu^2)}}} \rightarrow 0.13\ ns \leq \Delta t \leq 2.3\ ns \tag{24}$$

The time step, which was set to 1 ns, can also be checked in the DEM simulation by comparing it to the Hertz time and the Rayleigh time. In the LIGGGHTS documentation they are given by Equation (25) and (26) with the shear modulus G, the effective mass $1/m^* = 1/m_i + 1/m_j$, and the maximum velocity v_{max}:

$$\Delta t_R = \frac{\pi R \sqrt{\frac{\rho}{G}}}{(0.1631 * \nu + 0.8766)} \tag{25}$$

$$\Delta t_H = 2.87 * \left(\frac{m^{*2}}{R^* E^{*2} v_{max}} \right)^{\frac{1}{5}} \tag{26}$$

The number of time steps for the simulation was also decided. The particle was inserted a distance from the wall and it was given velocity components in x, y, and z direction for the particle to collide with the wall with a known impact angle and impact velocity. To enable efficient post-processing the particle was also made to collide with the wall at one specific time step and position, independent on the impact velocity and angle at collision.

Relevant ranges for impact velocity and impact angle were determined from CFD simulations. The work with CFD was performed by Enmark (2017) in a parallel master's thesis in the same overall research project. The simulations were performed both for a driving S90 car with snow particles injected at the surface of the tires, and a reference object with particles injected in front of it. Ranges for velocities and angles were taken from the rear part of the car and the reference object, since snow accumulated to larger extent in that region. Iteration of the DEM model was performed for a large setup of combinations of particle diameter, impact velocity, and impact angle. This was done in order to investigate under which circumstances a collision resulted in stick, and when the collisional outcome was bounce.

3.3.3 Modeling of collision with a rough wall

In reality a surface is never completely flat since all materials have some degree of surface roughness. This can be accounted for in a DEM model by replacing a flat wall (a sphere with infinite radius) with a rough wall. Modeling of rough walls can be done in different ways and one common strategy is to construct a lattice of particles (Kloss, 2016). This was implemented in the DEM model, with the same properties of the particles in the lattice as for the wall material (plastic). The particle

sizes in a plastic material were roughly estimated from microscope observation of a plastic radar cover. It was concluded that a suitable particle size for the rough surface was 1 µm. Particles were inserted within a defined volume with a volume fraction that of random close packing of spheres. However, in the DEM model the positions of the particles in the insertion are completely random, meaning that they are not packed but rather inserted randomly and are allowed to overlap. Therefore the volume fraction was increased to receive a suitable surface roughness of the wall.

3.3.4 Sensitivity analysis of particle properties

To investigate the influence of different input data to the DEM model, a sensitivity analysis of particle properties was performed. It included the ranges (minimum and maximum values) for properties found in literature, the range of work of adhesion calculated from the adhesion force determined through experiments by Abrahamsson (2017), as well as variation of the COR which was defined as a function of the yield stress and the normal impact velocity.

3.4 Post-processing of DEM model

From DEM simulations performed with LIGGGHTS it is possible to store information on particles in output text files. The type of information stored is defined by the user and can include for instance particle coordinates, velocity components, force components, and angular velocity components. Thereby it is possible to track a particle by storing information continuously for every time step or a defined interval between time steps. During the simulations in the thesis, output files were generated continuously for an interval between time steps. This was done for many iterations of the DEM model with a single particle colliding with a wall, and all iterations were given unique combinations of particle diameter, impact velocity, and impact angle. In order to visualize the simulations, the output files were converted from text format into VTK format. This enabled post-processing in the software ParaView which is an open-source application used for scientific visualization. With ParaView it was possible to display the time steps after each other for particle simulations and track the particles pre, during, and post collision.

The main goal with the post-processing in ParaView was to visualize particle-wall collisions and examine if the result of a collision was stick or bounce. For a great number of combinations of particle diameter, impact velocity, and impact angle, it is extremely time consuming to examine collisional outcome by visualization. To make the post-processing more efficient the output text files were opened and read in MATLAB. The particles were made to collide in a specific position and time step, which was described earlier, hence it was possible to read information of the particle coordinates at collision and compare with the coordinates an arbitrary time after collision. If a particle had the same coordinates at collision and after collision the particle stuck to the wall, otherwise bounce was the outcome of the collision.

3.5 VCC climatic wind tunnel

During the field study in northern Sweden cars were driven on snowy roads to investigate the build-up of snow on the exterior. In addition to field tests, wind tunnel experiments are performed at VCC to study contamination amongst other things. This test method has excellent repeatability, due to the controlled environment, compared to outdoor field tests. Therefore, validation of CFD simulations with wind tunnel experiments can be made efficiently. In this thesis snow adhesion experiments were performed in the climatic wind tunnel at VCC with an S90 car as well as a reference object. The purpose of the reference object was to have a less complex geometry, which

lowered the computational effort in the development of the snow adhesion CFD model that was performed in the parallel master's thesis (Enmark, 2017).

3.5.1 Reference object

Running unsteady CFD simulations of air-particle flows around a large and complex geometry, such as a full scale car, is time consuming. The mesh for the S90 car used in the CFD simulations by Eng et al. (2017) contains approximately 200 million cells, making it inconvenient for use in the development stage of a CFD model or a boundary condition. A reference object with a much more straight forward geometry was therefore created at VCC. The object was shaped like a wedge in order to get flow separation that creates a wake behind the object. It was also desired to have a flat surface on the rear side to be able to distinguish snow adhesion properly and compare with snow adhesion on the rear part of a car. Both a virtual and a physical model were built to enable CFD simulations and experiments in the wind tunnel (Figure 10).

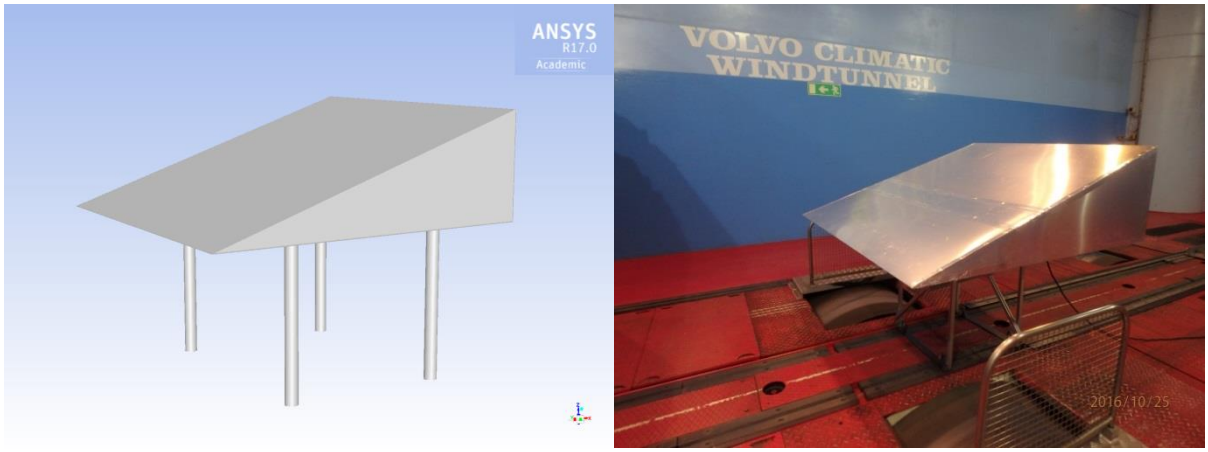

Figure 10. Virtual and physical model of the reference object that was used for CFD simulations and wind tunnel experiments.

3.5.2 Snow adhesion test

During the snow-build up tests for the S90 car and the reference object the temperature in the wind tunnel was around -15 °C. To simulate driving conditions, the wind tunnel air speed was put to 70 km/h and water was injected through nozzles in front of the test objects. When running the wind tunnel the water instantaneously freeze, forming tiny ice particles similar to the particles investigated in northern Sweden. The snow build-up experiments were run for 30 min and pictures were taken afterwards to be able to make comparisons with CFD simulations. For this master's thesis only the reference object was used for validation.

3.5.3 Increased temperature and humidity test

As described in the theoretical background the temperature and humidity greatly affects the snow characteristics. To investigate the influence of increased temperature on the snow build-up, experiments were conducted with heating pads placed on the inside of the rear surface of the wedge. The heating pads were connected to a small computer (Arduino) and a PID controller was used to set a fixed temperature closer to the melting point of ice. The heating pads were placed in two different locations; where a lot of snow accumulated and where little to no snow accumulated. Increased humidity was also tested by placing a steamer that injected water vapor in the wake behind the reference object. However, no significant effect was obtained from either of the two experiments mentioned and it will therefore be left out for the remainder of the thesis.

4. Results

This section will present the different results obtained. First of all the properties used as input data to the DEM model are summarized. The methodology to develop a regime map for particle stick or bounce is then described. Three variables were initially used to parameterize the regime map; impact angle, impact velocity, and particle diameter. The values of the variables were normalized due to confidentiality reasons. The influence of impact angle was, however, not successfully examined with the DEM model at the current stage. Instead the parameterization was made with normal velocity and particle diameter. A sensitivity analysis of particle properties was made to examine their effect on the results, and the findings will be illustrated in this chapter. The results from modeling of a rough surface will then be presented. Finally this chapter will show results from the validation of the DEM model, which included wind tunnel experiments of the reference object as well as CFD simulations of the reference object performed at VCC in the parallel master's thesis (Enmark, 2017).

4.1 DEM input data

The properties used as input data for the DEM model included Young's modulus, Poisson's ratio, work of adhesion, COR, and friction coefficients for sliding and rolling. In the simulations the impact angle, the impact velocity, and the particle diameter were varied in order to create regime maps for stick and bounce. Friction in terms of both sliding and rolling was unsuccessfully modeled with DEM as will be discussed in subsequent sections. The properties deemed most valid for the DEM model, referred to as the baseline values, as well as the range for the properties found in experiments and literature are summarized in Table 3. Extreme values found for all properties were used in a sensitivity analysis to validate the reliability of the DEM model.

Table 3. Properties deemed most valid for the DEM model as well as value ranges for the properties.

Property	Baseline value	Value range
Young's modulus [GPa]	**9.8**	**8.9-11.2**
Poisson's ratio [-]	**0.31**	**0.29-0.36**
Work of adhesion [J/m^2]	**0.2**	**0.1-1**
Yield stress [MPa]	**1**	**0.5-1.5**

The yield stress was in this thesis used for calculation of e_n (COR) which is presented and further explained in Appendix A.2. For the baseline value of the yield stress, seen in Table 3, e_n as a function of normal velocity was determined which is shown in Figure 11 below. In Appendix A.2 different correlations were used for particle-particle and particle-wall interaction. The difference in e_n for the two cases was deemed insignificant. Therefore e_n derived for particle-wall interaction was used for all cases. In the sensitivity analysis a lower and a higher value for the yield stress, see Table 3, were used to investigate the effect of e_n.

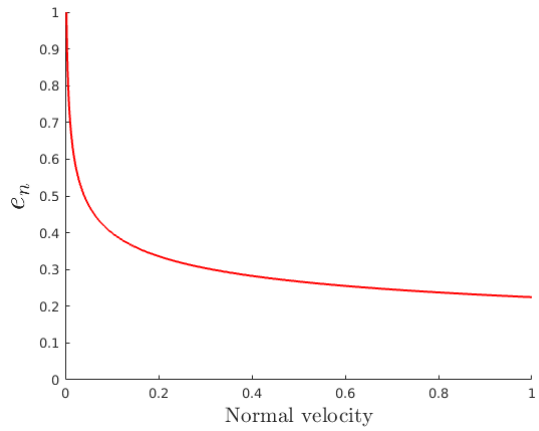

Figure 11. Normal COR, e_n, as a function of the scaled impact velocity in normal direction. e_n was calculated using a correlation for particle-wall interaction.

4.2 Regime map for particle stick or bounce

As the initial step to parameterize a regime map for particle stick or bounce, three variables were investigated; the particle diameter, the impact velocity, and the impact angle. The approach to set the criterion for particle stick, as explained in the post-processing part of the methodology, was to compare the particle coordinates at two different time steps after collision. If the coordinates were unchanged, the collisional outcome was to be regarded as stick.

In the DEM model a modified version of the Hertz contact model was used as described in the methodology. It was found that with this model it was unfeasible to study the influence of impact angle for collision of a spherical particle with a flat wall. This was because when a particle with normal and tangential velocity components adhered to the wall in the normal direction, the particle continued to slide along the wall in the tangential direction after collision. With a coefficient of friction within reasonable magnitude according to literature, particles were found to lose some of its tangential kinetic energy in a collision due to friction. However, particles were never found to lose all their tangential kinetic energy and completely stick to the wall. This will be discussed in the coming chapter.

Since the frictional force was not found to be large enough for particles not to slide, the criterion used in the development of the regime map for particle stick or bounce was instead only based on the normal overlap after collision. If the distance between the particle center and the wall is smaller than the particle radius, there is a normal overlap. Hence the particle coordinates were examined after collision to see if the particle had stuck to the wall. A three-dimensional regime map was obtained by checking the sticking criterion for different combinations of velocity magnitude, impact angle and particle diameter. The regime map is shown in Figure 12 where every dot is a particle with different combinations of the three parameters. If there was a normal overlap after collision the particle was given a red color representing stick, while the blue dots represents bounce for particles with no normal overlap after collision. Figure 13 shows the interface between stick and bounce with the green dots.

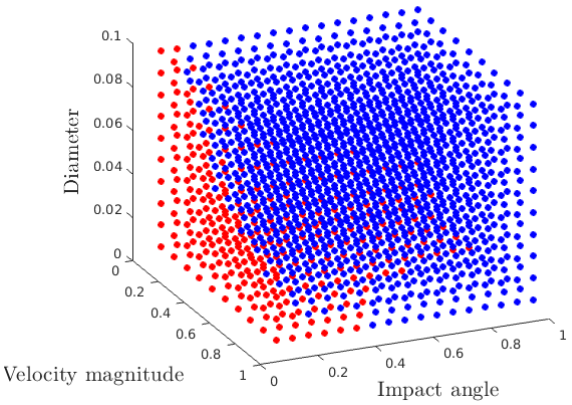

Figure 12. Regime map with scaled values of impact angle, velocity magnitude, and diameter. Red dots represent particle stick and blue dots represent particle bounce.

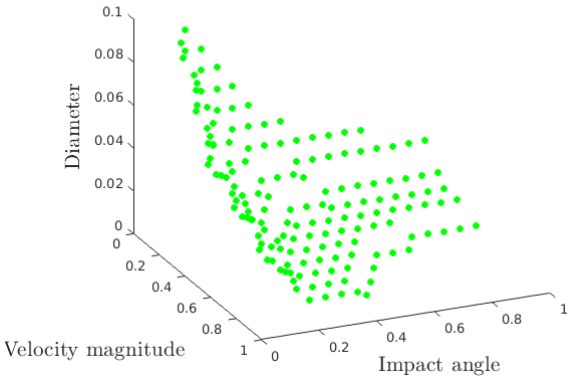

Figure 13. Regime map with scaled values of impact angle, velocity magnitude, and diameter. The green dots are plotted in the interface between stick and bounce.

In the DEM model the normal contact force, and hence the normal overlap, is not affected by the tangential velocity but only by the normal velocity of the particle. This is explained by the equations for the normal contact force presented previously in the theoretical background. It was also investigated by creating a regime map for normal velocity versus impact angle for a single particle diameter of 0.01 (scaled value), seen in Figure 14. The impact angle was therefore not further investigated in the DEM model with a flat wall. Instead the model was adjusted to parameterize a regime map with combinations two remaining variables; the normal velocity and the particle diameter. The result for the input data deemed most valid and normalized particle diameters of 0.01-0.1 is shown in Figure 15. Every dot in the regime map is a particle with a unique combination of normal velocity and particle diameter, where red dots represent particle stick and blue particle bounce. A clear difference in the sticking velocity can be seen for the smallest and the largest particle sizes investigated as seen in Figure 15. The smallest particles stick up to a normal velocity of about 0.5 on a normalized scale, while larger particles bounce at collision at the same velocity.

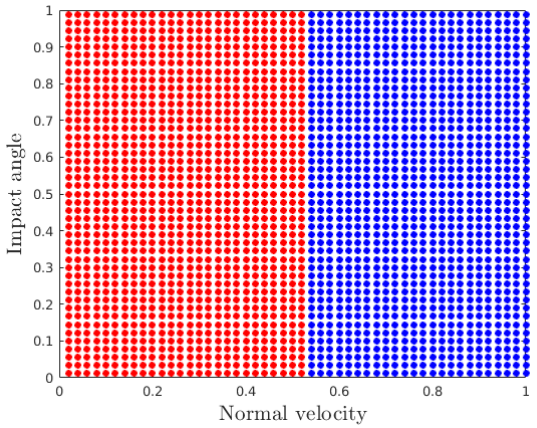

Figure 14. Regime map for scaled values of normal velocity and impact angle with a particle diameter of 0.01.

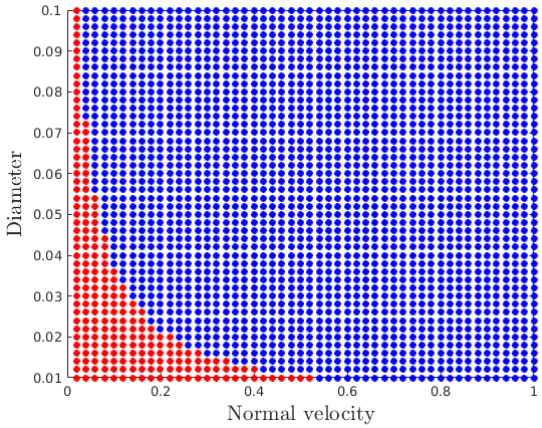

Figure 15. Regime map for scaled values of normal velocity and particle diameter with the baseline values in Table 3.

4.3 Sensitivity analysis of particle properties

In order to investigate what input data that influenced the result, a sensitivity analysis of particle properties was performed. It included the extreme values given in Table 3 for the Young's modulus, the Poisson's ratio, the work of adhesion, and the yield stress. The yield stress was, as mentioned before, used to calculate the COR. The same simulation setup as in Figure 15 was used, which

corresponded to 46 different particle diameters and 50 normal velocities (2300 combinations). For the lowest and highest literature values of the Young's modulus, no significant difference was found for the stick/bounce behavior. The result is shown in Figure 16 and Figure 17 respectively. A similar result was obtained for simulation of the extreme values found in literature for the Poisson's ratio. By evaluating the number of collisions that resulted in particle stick, the influence of the Poisson's ratio was even smaller than the Young's modulus. For the baseline case, seen in Figure 15, the number of collisions resulting in particle stick was 217. The Young's modulus of 8.9 GPa had 222 sticking collisions (Figure 16) while the Young's modulus of 11.2 GPa had 215 (Figure 17). No change compared to the baseline case was found when varying the Poisson's ratio (Figure 18, Figure 19).

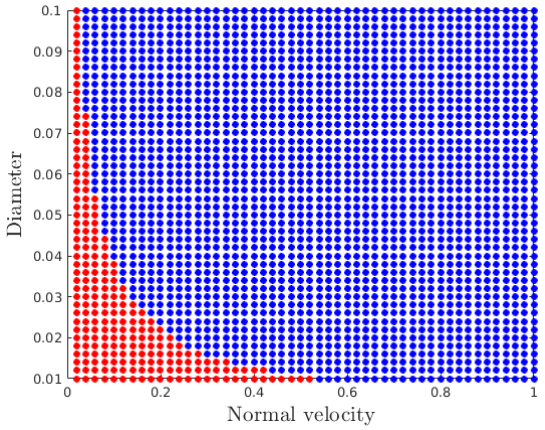

Figure 16. Regime map for scaled values of normal velocity and particle diameter with Young's modulus of 8.9 GPa.

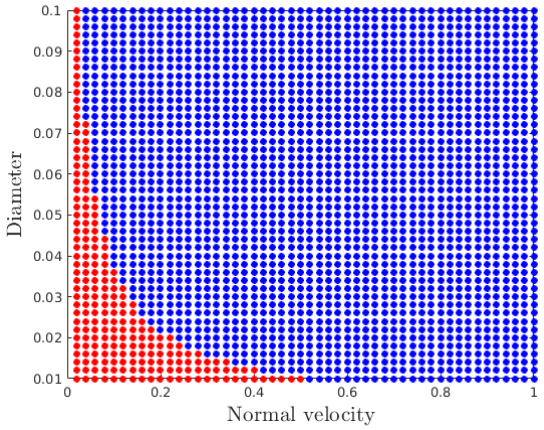

Figure 17. Regime map for scaled values of normal velocity and particle diameter with Young's modulus of 11.2 GPa.

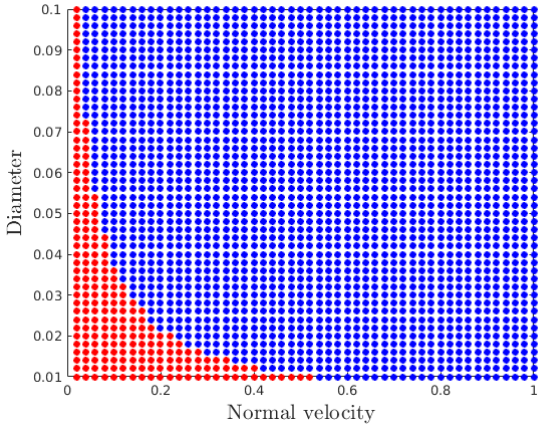

Figure 18. Regime map for scaled values of normal velocity and particle diameter with Poisson's ratio of 0.29.

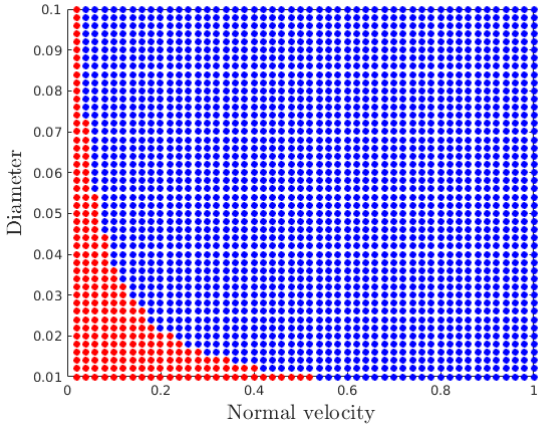

Figure 19. Regime map for scaled values of normal velocity and particle diameter with Poisson's ratio of 0.36.

As for the work of adhesion, using the minimum and maximum values from the experiments showed to give significant effect on the result. For the lowest value, 0.1 J/m^2, 71 particle collisions resulted in stick while for the highest value, 1 J/m^2, the number of sticking collisions was 1283. The result is shown below in Figure 20 and Figure 21 respectively. Uncertainty in this parameter, occurring either from the experimental procedure or from the mathematical derivation, will greatly influence the outcome of the stick or bounce regime map. The sensitivity for the COR in the DEM model was investigated by using a lower and a higher value for the yield stress. With a lower yield stress of 0.5 MPa the COR decreases, leading to an increase of energy dissipation due to plastic deformation. Particles thus stick to larger extent, as seen in Figure 22 where 512 particles stick. With a higher yield stress the yield velocity increases, hence a higher velocity is required for plastic deformation to occur

according to Equation (31,32) in Appendix A.2. Since less energy is dissipated due to plastic deformation with a higher yield stress, fewer particles stick (88 particles) which is shown in Figure 23.

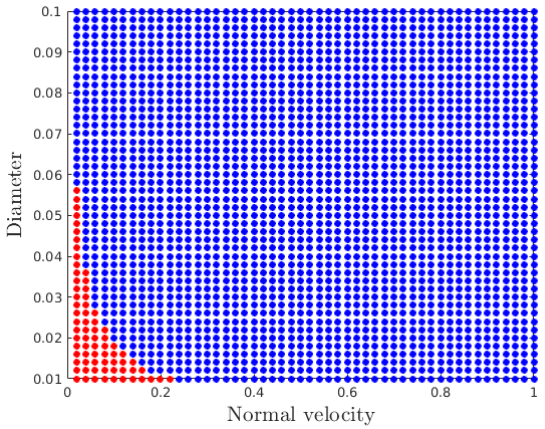

Figure 20. Regime map for scaled values of normal velocity and particle diameter with work of adhesion of 0.1 J/m^2.

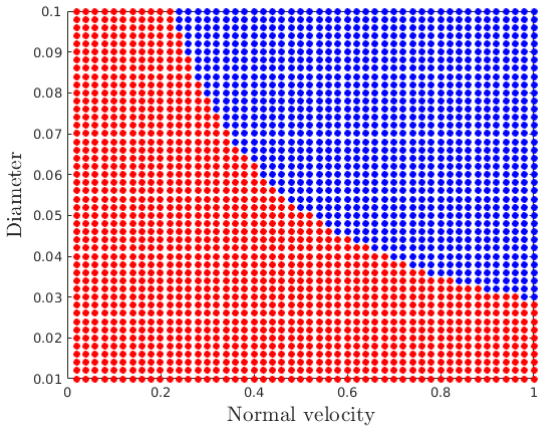

Figure 21. Regime map for scaled values of normal velocity and particle diameter with work of adhesion of 1 J/m^2.

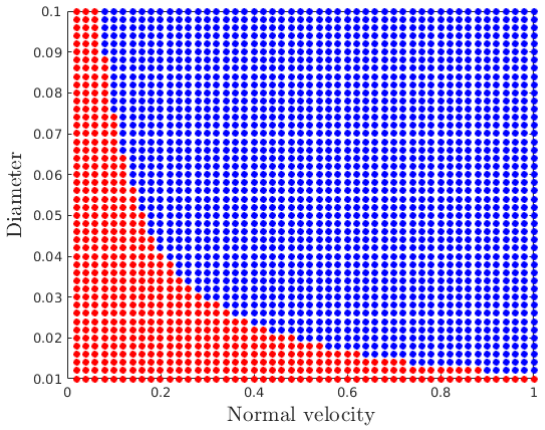

Figure 22. Regime map for scaled values of normal velocity and particle diameter with e_n for a yield stress of 0.5 MPa.

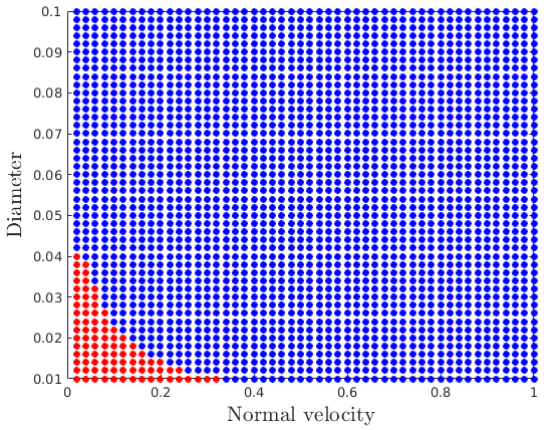

Figure 23. Regime map for scaled values of normal velocity and particle diameter with e_n for a yield stress of 1.5 MPa.

4.4 Rough wall model

In addition to simulation of particle collisions with a flat wall, a DEM model was created with a rough wall. This was done for several reasons. Firstly, materials are not completely smooth in reality and through modeling of a rough wall the effect of surface roughness could be investigated. Secondly, the impact angle dependence was thought to be more realistically modeled. And lastly, when snow builds up on a surface the snow-snow interaction becomes important which can be modeled as a rough surface of snow particles. For modeling of particle collision with a plastic material, the rough surface in Figure 24 was created. The particles in the wall were given the properties of plastic, and the volume fraction of random close packing of spheres was considered. Difficulties were met with obtaining a correct volume fraction with the method that was used, since the particles were inserted at random positions while having the ability to overlap.

The result from a simulation of particle collisions with the rough wall is shown in Figure 25. A particle diameter of 0.01 on a normalized scale was used and the impacts were normal towards the surface. For every normal velocity, simulations of multiple particle collisions at randomized positions on the rough wall were performed to get a statistical average of the collisional outcome. It was seen that compared to the simulations performed with a flat wall, sticking was obtained for much lower

normal velocities on a normalized scale. For the regime map of a flat wall with the baseline values, seen in Figure 15, sticking for a particle diameter of 0.01 was seen up to a normal velocity over 0.5 on a normalized scale between 0 and 1. For the rough surface with the same input data, particle stick was only obtained for a normal velocity of 0.04 on the normalized scale between 0 and 1. This can be explained by the lower contact area that arises between an ice particle and a particle in the rough wall, compared to an ice particle and a flat wall. The smaller contact area is obtained since it depends on the radii of both particles in a contact, as seen in Equation (17) in the theory of JKR.

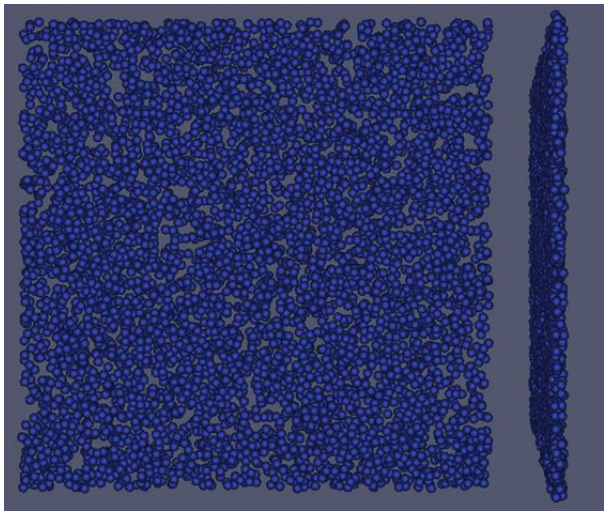

Figure 24. Front and side perspectives of the rough surface made of plastic particles with 1 µm diameters.

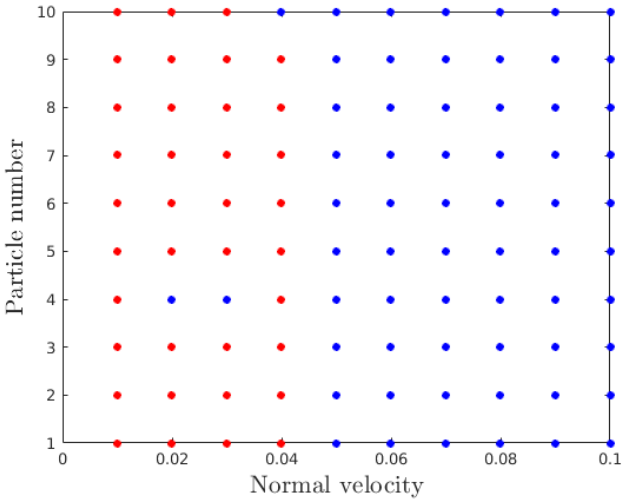

Figure 25. Regime map for particle collisions with normal impact on the rough surface.

4.5 Validation of the DEM model

For validation of the snow-wall adhesion model, wind tunnel experiments were performed in Volvo climatic wind tunnel. Tests were made both with the reference object as well as with an S90 car. For this thesis though, only the reference object was used for validation. The methodology of the validation was to run snow build-up tests and examine the outcome and document the results to enable comparison with simulations later on. CFD was used to run simulations of the reference object with a boundary condition developed for snow-wall adhesion. The results from the CFD simulations were then compared to the results from the wind tunnel tests. The CFD simulations and the development of a snow adhesion boundary condition were performed in the parallel master's thesis (Enmark, 2017).

4.5.1 Use of regime map in CFD simulations

The approach to use the results from the DEM model in CFD simulations was to implement the stick/bounce criterion from the regime map as a boundary condition via a user-defined function (UDF). For the baseline values in this study, the regime map was shown in Figure 15. To use the information from the regime map in a UDF an interface was created between stick and bounce according to Figure 26 where particles bounce to the right in the figure while particles stick to the left. A polynomial curve was then fitted to the interface between stick and bounce as seen in Figure 27. The UDF can then for every particle check the diameter and the normal velocity at collision. The particle diameter can then be compared to the diameter retrieved if the normal velocity when used as input to the function of the polynomial. If the particle diameter is larger than the diameter calculated in the polynomial the particle should bounce.

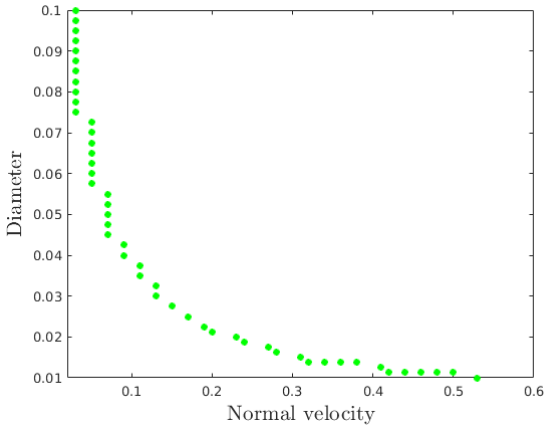

Figure 26. Dots plotted in the interface between stick and bounce.

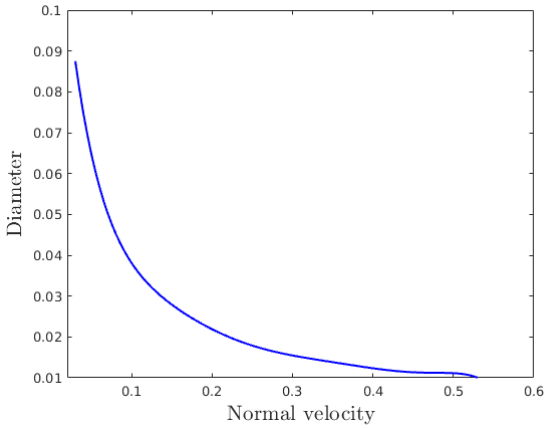

Figure 27. Polynomial curve fitted to the interface between stick and bounce.

The same procedure could be implemented for other parameterizations, e.g. a two variable regime map with velocity magnitude and impact angle or a three variable regime map that also includes the particle diameter.

4.5.2 Comparison of wind tunnel experiments and CFD simulations

From the field tests in northern Sweden the snow build-up was, as seen in Figure 28, much more apparent on the rear side of the car compared to for instance the side. For validation in this thesis the rear side of the reference object was therefore primarily considered for comparison with the CFD simulations. From the snow build-up test in the wind tunnel, which was described in the methodology, the pattern of the snow accumulation on the rear surface of the reference object is shown in Figure 29. Different parameters were investigated using CFD to understand their effect on where particles stick; including the normal velocity, tangential velocity, and angle for impact of parcels. The aerodynamic shear stress was also thought of as an important variable due to the rip off effect of snow accumulated on the exterior. Contour plots of the variables are shown in Appendix B, where Figure 33, Figure 34, and Figure 35 are for parcel impacts and Figure 36 is the surface shear stress.

Figure 28. Snow build-up test in northern Sweden of an S90 car.

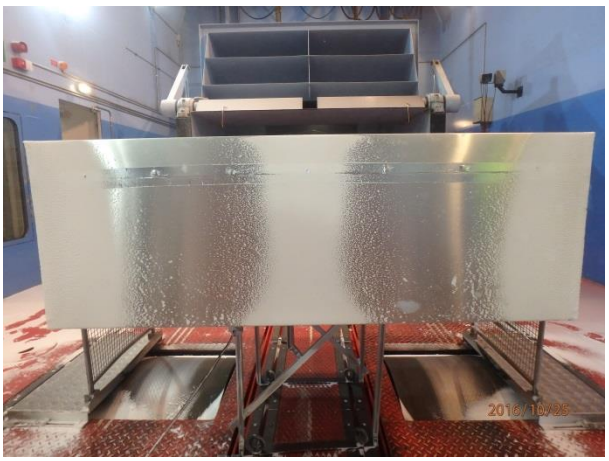

Figure 29. Reference object after 30 min of snow build-up with a wind speed of 70 km/h at -15 °C air temperature.

A boundary condition was developed by Enmark (2017) for ANSYS Fluent using a UDF. For a specific particle diameter, it was tested to base a boundary condition for particle collision purely on the

result from the regime map. The criterion for stick and bounce was that a normal velocity higher than the maximum sticking velocity gives bounce, while a lower velocity gives stick. It was found, however, that basing the boundary condition solely on the normal velocity was insufficient to describe the snow adhesion on the reference object. Therefore, the tangential velocity was added as an additional condition. This condition for stick and bounce was based on a tangential velocity contour plot (Figure 34 in Appendix B), which was compared to the pictures of snow build-up in the wind tunnel. The result for the boundary condition is shown in Figure 30 which had a sticking condition for the normal velocity according to the DEM regime map and a sticking condition for the tangential velocity according to comparison of pictures from CFD and the wind tunnel.

The picture from snow build-up on the reference object in the wind tunnel, as was shown previously in Figure 29, was compared to the result from the boundary condition in CFD. It can be seen that in Figure 29 snow particles stick on each side of the rear surface as well as in the center region. Also, as seen more in detail in Figure 31 down below, snow build-up was obtained on the edges of the reference object. While snow accumulation on the sides and center region on the rear surface was captured with CFD, the snow build-up on the edges was not seen with the sticking velocity from the DEM regime map.

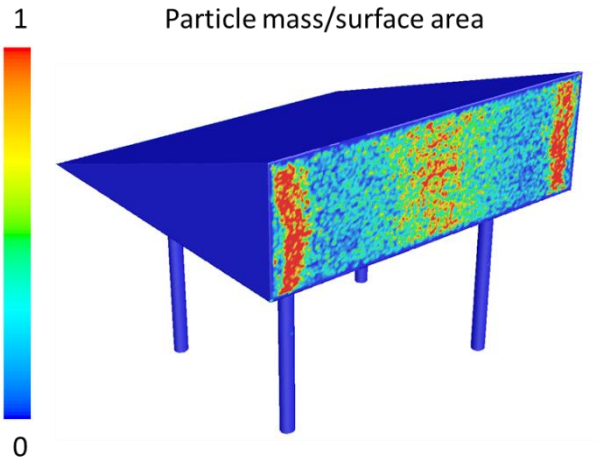

Figure 30. Contour plot of the face area particle mass (scaled).

Figure 31. Image of snow build-up on the edges of the reference object.

5. Discussion

This chapter will begin with a discussion of the particle properties used in the DEM model. Assumptions made in the thesis are mentioned as well as the disadvantages with deriving properties analytically instead of performing experiments. The shortcomings of the DEM model will then be mentioned. Approaches to use the developed DEM model and the framework for creating regime maps will also be discussed, particularly about using other parameterizations and models for other snow types. This chapter will finally bring my suggestions for further work.

5.1 Particle properties

An assumption made for the DEM model was that the particles were perfectly spherical. In reality the snow particles are non-spherical and most likely they also have structural defects. The particle characteristics used in the model in terms of the density and the mechanical properties are valid for a case with perfectly spherical solid ice particles. To make the model represent the snow particles that accumulate on cars in the field, more experiments to determine the particle properties have to be performed. The experiments performed up to this point have decided the PSD as well as adhesive force. Uncertainty still remains when it comes to deriving the work of adhesion from the adhesion force. This is due to the fact that the device used for the experiments was not capable of measuring the adhesion force of a single particle but rather for snow particle agglomerates. The procedure to use the adhesion force of an agglomerate to estimate the force for a single particle was ambiguous.

Within the suggested range of the Young's modulus and the Poisson's ratio from literature, small differences were found for the regime maps. The work of adhesion and the COR on the other hand showed to have significant impact on the regime map result. The methodology behind deriving the COR was not straight forward and a particle yield stress was required. Commonly the yield stress depends both on the conditions during the test as well as the measurement technique. Therefore it would to my belief be a better approach to define the COR by experiments instead of deriving it analytically from material properties. Measurements to determine the COR for ice spheres have been performed previously (Higa, et al., 1996). The velocities pre and post collision were obtained either with a high speed camera or with sensors to measure acoustic emission signals. The measurements were performed with an ice sphere with a diameter of 1.5 cm which is much larger than the ice spheres considered in the DEM model in this thesis. To perform experiments to determine the COR for the particles considered in this thesis, equipment with very high precision is required.

For investigation of impact angles the force of friction becomes important. In order to model friction with DEM, sliding and rolling friction coefficients have to be determined. Mills (2008) states that the static and kinetic friction coefficients of ice are typically around 0.05. Naturally the friction coefficients do not only depend on the properties of snow or ice, but also on the material that is modeled as the wall.

5.2 Shortcomings of the DEM model

The DEM model was developed to qualitatively simulate the particle collisions that take place during snow build-up on cars. Before adding complexity to the problem it is essential to capture the fundamental mechanics of particle interactions. In this thesis the focus was consequently put into

finding as reasonable properties as possible and to efficiently validate the collisional outcomes by development of a regime map. With the simplifications that were made, there are several phenomena that remain left out in the model. Apart from the non-ideal particle structure which was discussed in the previous section, the most crucial one at this stage is considered to be realistic modeling of friction.

With the contact model used in this thesis the friction is modeled with a shear force and a damping force. The shear force, which corresponds to a tangential spring, is modeled as a history effect that takes the tangential overlap of the contact into account. Both the shear and dampening forces are functions of material properties, and the tangential force grows in particle interactions until the upper limit of the Coulomb criterion in Equation (4) is reached. This is when the tangential force equals the normal force times the coefficient of friction μ (Kloss, 2016). For the interaction between a particle and a flat wall modeled in this thesis it was found that the friction dampened the tangential kinetic energy during collision, while the particle continued to slide along the wall after a collision that resulted in stick in the normal direction.

In order to investigate the effect of impact angle, a more reasonable friction model has to be implemented. With sliding (kinetic) and rolling friction coefficients the criterion for stick can then be based on two things: if there is a normal overlap after collision and if the tangential coordinates of the particle are unchanged i.e. that a static contact is obtained. For a perfectly spherical particle, sliding and rolling along a flat surface will not result in that the particle leaves the surface. This is because the normal and tangential contact forces are calculated independently on each other, and there is no contribution to the normal force when a spherical particle slides or rolls on a flat wall. In reality however, an inhomogeneous structure of the particle and/or the surface can lead to a normal force contribution. Therefore it is important to consider both the normal and tangential directions to define whether a particle collision should be regarded as stick or bounce.

A phenomenon that has not been included in the model is shear force. When a particle sticks to a wall, e.g. snow on a car, shear forces from a fluid flow can pull the particle of the surface. Using LIGGGHTS a simple force field can be included in the DEM model, while modeling of a continuous fluid flow is performed with CFD. Coupling between the DEM model and CFD is possible but the computational effort is extensive for transient simulation with many particles (Kloss, et al., 2012). Therefore the shear force could be investigated in DEM as a simplified applied force, and it may be possible to use the information to create a regime map to be implemented in CFD.

5.3 Parameterization of regime map

The approach to parameterize the regime map was initially to include impact angle, impact velocity, and particle. Since it was found difficult to evaluate the impact angle, the remaining two variables were used to span the regime map and to make a sensitivity analysis of input data to the DEM model. With the developed framework though, it is possible to use other parameterizations for the regime maps. If more reasonable modeling of friction is included the impact angle can be investigated. For a rough surface, where impacts depend on where the particles collide due to asymmetry, multiple runs can be made to retrieve a statistical average. It is hence possible to include more variables for the stick or bounce criterion to be used as boundary condition for the CFD simulations. It is, however, more difficult to use the information from a regime map if more than two variables is used. For a 2D

case a function can be fitted to the interface between stick and bounce. For a 3D map, it was tested to fit a plane instead but that procedure is not as straight forward.

5.4 Modification of DEM model for other snow types

The current DEM model was created for particles where van der Waals interaction is the dominant adhesive force. Depending on the ambient conditions, mainly the temperature and the humidity, the attractive forces may instead be governed by capillary forces originating from liquid bridges created between bodies. This type of adhesion is much stronger than the van der Waals force and becomes relevant when water is present around and between particles. For snow particles close to 0 °C and/or at high humidity (unlike the dry snow from northern Sweden) a contact model for capillary forces should therefore be used instead of the JKR model. This modification can be implemented in the DEM model and there are two existing models for capillary forces in the LIGGGHTS framework.

Temperature and humidity also affect the physical properties of snow particles. While changing the particle properties and the contact models in the DEM model is achievable, it is more challenging to find the correct properties and models. The field of characteristics of snow particles is relatively untouched, thus experiments have to be performed to determine the properties. Due to the complexity of particle contacts and collisions, the choice of contact model and its derivation should always be validated. When it comes to capillary forces for instance, there are two models available in the existing framework of LIGGGHTS. There are different assumptions made in the models and it is important to understand the differences. Gladkyy & Schwarze (2014) investgated the different theories for capillary bridge models. The models were implemented in DEM and the simulations were compared with experimental measurements. Likewise, experiments have to be performed to validate the choice of contact model for different snow types.

5.5 Suggestions for further work

With the current DEM model, a friction coefficient within reasonable range was not large enough to keep particles from sliding along a wall. I suggest that the way friction is modeled should be looked into in the future work. Also the sliding and rolling friction coefficients for the model should be determined, either from similar studies in literature or from experimental trials. If friction can be modeled successfully the impact angle dependence can be investigated for particle stick or bounce.

Modeling with a rough surface was performed since it affects both the impact behavior and the particle contacts. Thereby collision could be modeled more realistically, and a rough surface will be even more important for modeling of snow-snow interaction where the particles are of equal size. This thesis focused on modeling of snow-wall adhesion, which is the initial mechanism for accumulation of snow on cars. When the snow continues to build up the snow-snow interaction will be the governing mechanism, thus making modeling with a rough surface vital. Effort then has to be put into determining the characteristics of snow-snow interaction. Input data such as the COR and the work of adhesion should be investigated experimentally.

Finally my recommendations for future studies include continued work with the DEM model and the regime map. For the DEM part, extending the model for other snow types is an important step to be able to predict snow accumulation more universally. In order to make a regime map that can predict snow contamination, other variables have to be included. Impact angle as well as shear forces are considered to be interesting variables to evaluate and use in parameterization of regime maps.

6. Conclusions

Input data to the DEM model for the snow particles and the wall material included Young's modulus, Poisson's ratio, coefficient of restitution, work of adhesion, and particle size distribution. Appropriate ranges for the properties were found either in literature or from experiments that were performed in the same overall project prior to this thesis. The JKR model was implemented to account for adhesive interaction in the DEM model and the legitimacy of this model was estimated using the Tabor parameter. Different variables were investigated in the DEM model to study particle collisions. To create a regime map for stick and bounce, parameterization with combinations of the normal velocity at collision and the particle diameter was made. Other important variables, primarily the impact angle, were examined but were not further used due to unreasonable modeling of friction.

To study the reliability of the DEM model results a sensitivity analysis was performed for the input data. The work of adhesion as well as the coefficient of restitution showed to affect the results significantly. Within the range of values found for the Young's modulus and Poisson's ratio on the other hand, no major change was seen in the stick and bounce behavior. Modeling with a rough surface was performed by creating a particle lattice. Particle stick was found to occur at lower normal velocities due to the reduced contact area compared to interaction with a flat wall. Simulation of particle collisions with a rough surface becomes more important for snow-snow interaction, but this was not within the scope of this thesis.

Information from the regime map was used to create a snow adhesion boundary condition for CFD simulations. This was performed by fitting a polynomial curve to the interface between stick and bounce. For validation of the particle adhesion model, snow build-up tests were performed in Volvo climatic wind tunnel. The comparison between the CFD simulations and the wind tunnel test showed that it was insufficient to describe the impact behavior with only normal velocity. Parameterization with additional variables is therefore suggested as the next step in future work. The DEM model results in terms of the critical normal velocity for particle stick is deemed to be within relevant magnitude from the validation. Snow-snow interaction, which becomes important as snow accumulation progresses, can be implemented in the DEM model if properties for input data are found in literature or from experiments.

References

Abrahamsson, P., Eng, M. & Rasmuson, A., 2017. *An infield study of road snow properties related to snow-car adhesion and snow smoke,* s.l.: s.n.

Andersson, B. et al., 2014. *Computational Fluid Dynamics for Engineers.* 10th ed. Gothenburg: Cambridge University Press.

Bertrand, F., Leclaire, L. A. & Levecque, G., 2005. DEM-based models for the mixing of granular materials. *Chemical Engineering Science,* 60(8), pp. 2517-2531.

Cambridge University Engineering Department, 2003 Edition. *Materials Data Book.* [Online] Available at: http://www-mdp.eng.cam.ac.uk/web/library/enginfo/cueddatabooks/materials.pdf [Accessed 11 01 2017].

Colbeck, S. C., 1986. Classification of Seasonal Snow Cover Crystals. *Water Resources Research,* 22(9), pp. 59S-70S.

Crowe, C. T., Schwarzkopf, J. D., Sommerfeld, M. & Tsuji, Y., 2012. *Multiphase Flows with Droplets and Particles.* Second ed. s.l.:Taylor & Francis Group, LLC.

Cundall, P. A. & Strack, O. D. L., 1979. A discrete numerical model for granular assemblies. *Geotechnique,* 29(1), pp. 47-65.

Eng, M., Sterken, L. & Abrahamsson, P., 2017. Unsteady CFD Particle Methodology for Snow Self-Contamination of a Passenger Vehicle.

Enmark, M., 2017. *CFD Modeling of Snow Contamination on Cars,* Göteborg, Sweden: Chalmers Publication Library.

Fierz, C. et al., 2009. The International Classification for Seasonal Snow on the Ground. *IHP-VII Technical Documents in Hydrology,* 83(1).

Fletcher, N. H., 1970. *The chemical physics of ice.* Cambridge: The University Press.

Fluent Theory Guide, Release 17.0. Discrete Phase. In: *ANSYS® Documentation.* s.l.:ANSYS, Inc.

Fluent User's Guide, Release 17.0. Modeling Discrete Phase. In: *ANSYS® Documentation.* s.l.:ANSYS, Inc.

Gaylard, A. P. et al., 2014. Insights into Rear Surface Contamination Using Simulation of Road Spray and Aerodynamics. *SAE International Journal of Passenger Cars - Mechanical Systems,* 7(2), pp. 673-681.

Gladkyy, A. & Schwarze, R., 2014. Comparison of different capillary bridge models for application in the discrete element method. *Granular Matter,* 16(6), pp. 911-920.

Hatzes, A. P., Bridges, F. G. & Lin, D. N. C., 1988. Collisional properties of ice spheres at low impact velocities. *Monthly Notices of the Royal Astronomical Society,* Volume 231, pp. 1091-1115.

Hertz, H., 1882. Über die Berührung fester elastischer Körper. *Journal fur die Reine und Angewandte Mathematik,* 1882(92), pp. 156-171.

Higa, M., Arakawa, M. & Maeno, N., 1996. Measurements of restitution coefficients of ice at low temperatures. *Planetary and Space Science,* 44(9), pp. 917-925.

Higa, M., Arakawa, M. & Maeno, N., 1998. Size Dependence of Restitution Coefficients of Ice in Relation to Collision Strength. *Icarus,* 133(2), pp. 310-320.

Jin, F., Zhang, C., Hu, W. & Wang, J., 2011. 3D mode discrete element method: Elastic model. *International Journal of Rock Mechanics and Mining Sciences,* 48(1), pp. 59-66.

Johnson, K. L., Kendall, K. & Roberts, A. D., 1971. Surface Energy and the Contact of Elastic Solids. *Proceedings of the Royal Society of London. Series A, Mathematical and Physical Sciences,* 324(1558), pp. 301-313.

Kloss, C., 2016. *LIGGGHTS(R)-PUBLIC Documentation,* Linz, Austria: DCS Computing Gmbh.

Kloss, C. et al., 2012. Models, algorithms and validation for opensource DEM and CFD-DEM. *Progress in Computational Fluid Dynamics,* 12(2-3), pp. 140-152.

Kosinski, P. & Hoffmann, A. C., 2011. Extended hard-sphere model and collisions of cohesive particles. *Physical Review E - Statistical, Nonlinear, and Soft Matter Physics,* 84(3).

Krijt, S. et al., 2013. Energy dissipation in head-on collisions of spheres. *Journal of Physics D-Applied Physics,* 46(43).

Libbrecht, K. G., 2007. The Formation of Snow Crystals. *American Scientist,* 95(1), pp. 52-59.

Libbrecht, K. G., 2016. *SnowCrystals.com.* [Online]
Available at: http://www.snowcrystals.com/morphology/morphology.html
[Accessed 27 12 2016].

Li, S., Marshall, J. S., Liu, G. & Yao, Q., 2011. Adhesive particulate flow: The discrete-element method and its application in energy and environmental engineering. *Progress in Energy and Combustion Science,* 37(6), pp. 633-668.

Marshall, J. S. & Shuiqing, L., 2014. *Adhesive Particle Flow: A Discrete-Element Approach.* s.l.:Cambridge University Press.

Miller, D. A., Adams, E. E. & Brown, R. L., 2003. A microstructural approach to predict dry snow metamorphism in generalized thermal conditions. *Cold Regions Science and Technology,* 37(3), pp. 213-226.

Mills, A., 2008. The coefficient of friction, particularly of ice. *Physics Education,* 43(4), pp. 392-395.

Nakaya, U., 1954. Snow Crystals. *American Journal of Physics,* 22(8), p. 573.

Nguyen, D., Rasmuson, A., Thalberg, K. & Niklasson Björn, I., 2014. Numerical modelling of breakage and adhesion of loose fine-particle agglomerates. *Chemical Engineering Science,* Volume 116, pp. 91-98.

Petrovic, J. J., 2003. Mechanical properties of ice and snow. *Journal of Materials Science,* 38(1), pp. 1-6.

Professional Plastics, 2017. *Mechanical Properties of Plastic Materials.* [Online]
Available at:
http://www.professionalplastics.com/professionalplastics/MechanicalPropertiesofPlastics.pdf
[Accessed 11 01 2017].

Steinkogler, W. et al., 2015. Granulation of snow: From tumbler experiments to discrete element simulations. *Journal of geophysical research,* 120(6), p. 1107–1126.

Sterken, L., Sebben, S. & Löfdahl, L., 2016. Numerical Implementation of Detached-Eddy Simulation on a Passenger Vehicle and Some Experimental Correlation. *Journal of Fluids Engineering,* 138(9), pp. 091105-091105-14.

Tabor, D., 1977. Surface Forces and Surface Interactions. *Journal of Colloid and Interface Science,* 58(1), p. 2–13.

Thompson, C., 2016. *The 3 biggest ways self-driving cars will improve our lives.* [Online]
Available at: http://www.businessinsider.com/advantages-of-driverless-cars-2016-6/?r=US&IR=T&IR=T/#roads-will-be-safer-1
[Accessed 26 December 2016].

Thornton, C., 1997. Coefficient of restitution for collinear collisions of elastic-perfectly plastic spheres. *Journal of Applied Mechanics,* 64(2), pp. 383-386.

Thornton, C., 2015. *Granular Dynamics, Contact Mechanics and Particle System Simulations: A DEM study.* s.l.:Springer International Publishing.

Thornton, C. & Ning, Z., 1998. A theoretical model for the stick/bounce behaviour of adhesive, elastic-plastic spheres. *Powder Technology,* 99(2), pp. 154-162.

Vedachalam, V., 2011. *Discrete Element Modelling Of Granular Snow Particles Using LIGGGHTS,* Edinburgh, UK: Edinburgh Parallel Computing Centre, The University of Edinburgh.

Volvo Car Corporation, 2016. *Volvo Cars.* [Online]
Available at: http://www.volvocars.com/intl/about/our-innovation-brands/intellisafe/autonomous-driving/this-is-autonomous-driving
[Accessed 26 December 2016].

Appendix A

Appendix A.1

With the measured forces from the adhesion experiments performed by Abrahamsson (2017), the work of adhesion Γ was derived using correlations in the work of Thornton (2015). The apparent Hertzian force F_n^H was calculated using a function of the actual applied normal force F_n and the critical normal force F_{nc}:

$$F_n^H = F_n + 2F_{nc} + (4F_nF_{nc} + 4F_{nc}^2)^{\frac{1}{2}} \tag{27}$$

The relative surface curvature increases from R^* to R_p^* due to contact flattening. Thornton (2015) describes that R_p^* can be calculated using the equivalent Hertzian force F_n^{H*}, the applied load F_n^*, and the critical normal force F_{nc}:

$$R_p^* = \frac{R^* F_n^{H*}}{F_n^* + \sqrt{4F_{nc}F_n^{H*}}} \tag{28}$$

The work of adhesion Γ is then calculated using the equation of the critical normal force:

$$F_{ncr} = 1.5\pi\Gamma R_p^* \tag{29}$$

For dry snow from northern Sweden the work of adhesion was found to be within a range of 0.1-1 J/m^2. The mean value of the work of adhesion was 0.20 J/m^2.

Appendix A.2

In elastic collisions the COR has been reported to be fairly constant. For elastic-plastic interaction, the plastic deformation increases the kinetic energy loss and therefore a lower COR is expected (Thornton, 2015). Plastic deformation occurs when the contact area is affected by a limiting contact pressure p_y (Thornton, 1997). In the work of Thornton (1997), an interaction is divided into an elastic stage with a Hertzian pressure distribution and a plastic stage where the pressure distribution is described with a limiting contact pressure $p_y = 2.5\sigma_y$. Most materials can be described by a stress-strain curve where the material stops behaving elastically at the yield stress σ_y, and the tensile strength is the maximum stress that a material can withstand before breaking occurs. No yield stress was found in literature for ice, but Petrovic (2003) reported that the tensile strength for ice is in the range of 0.7-3.1 MPa. It was assumed the the yield stress σ_y is equal to 1 MPa.

The limiting contact pressure is with those assumptions:

$$p_y = 2.5 * 1 = 2.5\ MPa \tag{30}$$

The yield velocity V_y, which is the maximum relative velocity for a purely elastic collision, can be described by Equation (31) for a particle-particle interaction. With the rough surface, collision between an ice particle and plastic particles in the rough wall was modeled.

$$V_y = 3.194\left(\frac{p_y^5 R^{*3}}{E^{*4} m^*}\right)^{\frac{1}{2}} \tag{31}$$

For particle-wall interaction, which was modeled by collision of an ice particle and a flat plastic wall, V_y can be calculated as:

$$V_y = 1.56\left(\frac{p_y^5}{E^{*4}\rho}\right)^{\frac{1}{2}} \tag{32}$$

The COR, e_n, can be described as a function of the impact velocity V_i. For an ice particle impacting with a plastic particle in the rough wall, e_n is calculated by Equation (33) for impact velocities much higher than the yield velocity. For impact of an ice particle with a flat wall of plastic on the other hand, e_n can be calculated using Equation (34). For the range of impact velocities considered in this thesis, e_n is plotted against the normal velocity in Figure 32. Due to the small difference of e_n between the correlation for particle-particle and particle-wall interaction, the latter was used in the DEM model for all simulations.

$$e_n = 1.185\left(\frac{V_y}{V_i}\right)^{\frac{1}{4}} \tag{33}$$

$$e_n = 1.324\left(\frac{p_y^5}{E^{*4}\rho}\right)^{\frac{1}{8}} V_i^{-\frac{1}{4}} \tag{34}$$

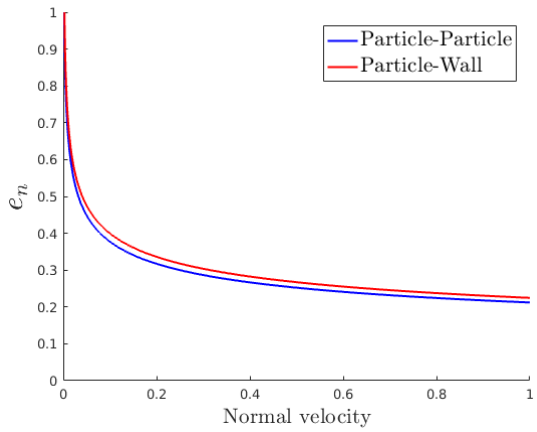

Figure 32. e_n as a function of normal velocity.

Appendix B

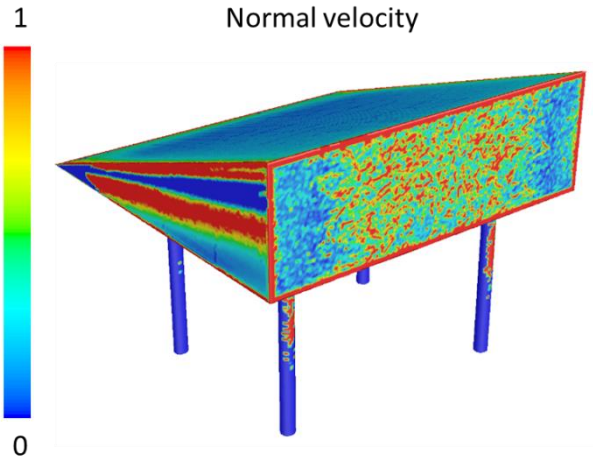

Figure 33. Contour plot of the normal velocity (scaled) for parcel collisions on the surface.

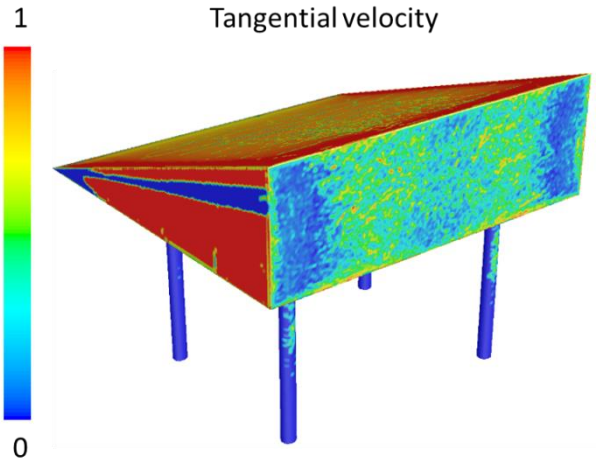

Figure 34. Contour plot of the tangential velocity (scaled) for parcel collisions on the surface.

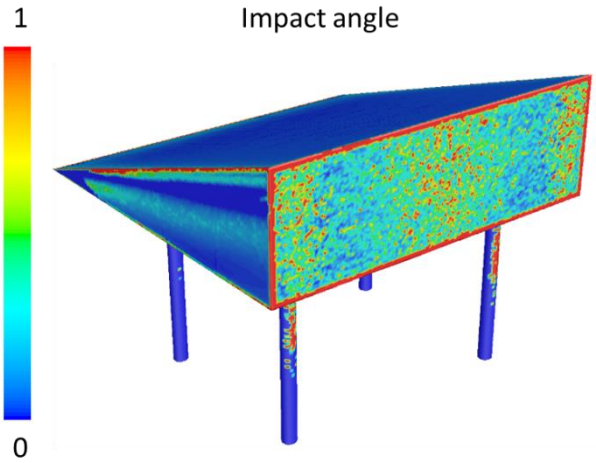

Figure 35. Contour plot of impact angle (scaled) for parcel collisions on the surface.

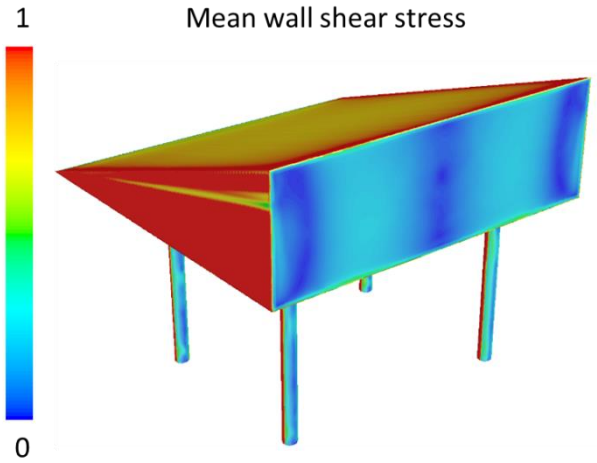

Figure 36. Contour plot of mean wall shear stress (scaled) on the surface.